ROCK-FLUID CHEMISTRY IMPACTS ON SHALE HYDRAULIC FRACTURE AND MICROFRACTURE GROWTH

A Thesis

by

ADERONKE ABIODUN ADERIBIGBE

Submitted to the Office of Graduate Studies of
Texas A&M University
in partial fulfillment of the requirements for the degree of

MASTER OF SCIENCE

May 2012

Major Subject: Petroleum Engineering

Rock-Fluid Chemistry Impacts on Shale Hydraulic Fracture and Microfracture Growth

ROCK-FLUID CHEMISTRY IMPACTS ON SHALE HYDRAULIC FRACTURE AND MICROFRACTURE GROWTH

A Thesis

by

ADERONKE ABIODUN ADERIBIGBE

Submitted to the Office of Graduate Studies of
Texas A&M University
in partial fulfillment of the requirements for the degree of

MASTER OF SCIENCE

Approved by:

Co-Chairs of Committee,	Robert H. Lane
	David Burnett
Committee Member,	Bryan Boulanger
Head of Department,	Dan Hill

May 2012

Major Subject: Petroleum Engineering

ABSTRACT

Rock-Fluid Chemistry Impacts on Shale Hydraulic Fracture and Microfracture Growth.

(May 2012)

Aderonke Abiodun Aderibigbe, B.Sc., University of Lagos, Nigeria

Co-Chairs of Committee: Dr. Robert Lane
Mr. David Burnett

The role of surface chemical effects in hydraulic fracturing of shale is studied using the results of unconfined compression tests and Brazilian tests on Mancos shale-cored at depths of 20-60 ft. The rock mineralogy, total organic carbon and cation exchange capacity were determined in order to characterize the shale. Adsorption tests to study the interaction of the shale and aqueous fluid mixture were also carried out using surface tension measurements.

The uniaxial compressive strengths and tensile strengths of individual shale samples after four hours exposure to water, $2.85x10^{-3}$M cationic surfactant (dodecyltrimethylammonium bromide- DTAB) and $2.81x10^{-3}$M anionic surfactant (sodium dodecylbenzenesulfonate-SDBS) were analyzed using ANOVA and Bonferroni tests. These mechanical strengths were largely reduced on exposure to the aqueous environments studied, despite the relatively low clay and low swelling clay content of the Mancos shale. Further comparison of the uniaxial compressive strengths and tensile strengths of the shale on exposure to water, to the strengths when exposed to the

surfactant solutions showed that their difference was not statistically significant indicating that exposure to water had the greatest effect on strength loss.

The surface tension measurement of 2.85×10^{-4}M DTAB and 2.81×10^{-4}M SDBS solutions before and after equilibration with shale showed about 80% increase in surface tension in the DTAB solution and 10% increase in surface tension in the SDBS solution. The probable sorption mechanism is electrostatic attraction with negatively charged sites of the shale as shown by significant loss of the cationic surfactant (DTAB) to the shale surface, and the relatively minor adsorption capacity of the anionic surfactant (SDBS). Although these adsorption tests indicate interaction between the shale and surfactant solutions, within the number of tests carried out and the surfactant concentration used, the interaction does not translate into a significant statistical difference for impacts of surfactants on mechanical strength of this shale compared to the impact of water alone.

The relevance of this work is to facilitate the understanding of how the strength of rock can be reduced by the composition of hydraulic fracturing fluids, to achieve improved fracture performance and higher recovery of natural gas from shale reservoirs.

DEDICATION

I dedicate my thesis to my family and friends.

ACKNOWLEDGEMENTS

I sincerely appreciate my committee chair and advisor, Dr. Lane, for his unflinching patience, guidance and support throughout my program. I particularly thank him for believing in me.

I am grateful to Mr. David Burnett and the Crisman Institute of the Petroleum Engineering Department for making available the funds for this work. I appreciate Dr. Boulanger for his advice and for serving as a member of my advisory committee. I thank the personnel at the Soil Characterization laboratory- Soil and crop science department; Rock Mechanics laboratory- Petroleum Engineering department; and Advanced Characterization of Infrastructure Materials (ACIM) laboratory- Civil Engineering department for the parts of this work they supported.

My colleagues and research group completed the invaluable experience of my program with the fun and combination of skills they exude, I am glad our paths crossed.

NOMENCLATURE

A	Specimen Area
CEC	Cation Exchange Capacity
CMC	Critical Micelle Concentration
CT	Computerized Tomography
D	Specimen Diameter
DTAB	Dodecyltrimethylammonium Bromide
E	Young's Modulus
H_1	Null Hypothesis Rejected
H_0	Null Hypothesis Accepted
M	Moles Per Liter
n	Number of Observations
P	Maximum Load Required to Fail the Specimen
SDBS	Sodium Dodecylbenzenesulfonate
s_p	Weighted Mean of Sample Variances
St	Tensile Strength
t	Specimen Thickness
TOC	Total Organic Carbon
UCS	Uniaxial Compressive Strength
$\overline{x}$	Mean
XRD	X-ray Diffraction

TABLE OF CONTENTS

CHAPTER Page

LIST OF FIGURES

FIGURE Page

LIST OF TABLES

CHAPTER I

INTRODUCTION

1.1 Statement of Problem

The chemistry interaction between shale and fracture fluids is yet to be completely understood, and this could contribute immensely to understanding the factors affecting enhancement of microfracture crack propagation and conductivity growth for improving hydraulic fracture performance. Improvements in microfractures generated during hydraulic fracturing of shales can lead to improved rates and recoveries from source rock resources. This work seeks to study effects of chemical environments (water and surfactants) on shale that can enhance fluid contribution to improvement of fracture growth.

Studies of the effect of surfactants on individual mineral samples and sandstones have shown that surfactants cause a reduction in the bonding forces across the developing crack or fracture as a result of adsorption of the surfactant on the surface, hence altering the materials' surface energy, according to the Rehbinder model. Some studies have also proposed that the zeta potential of fluid environment affects the mobility and nucleation of dislocations at or near the surface of the material, and inhibits or improves the growth of brittle cracks or fractures, according to the Westwood model.

This thesis follows the style of *SPE Productions and Operations Journal.*

Other studies on micromechanisms of fracturing and subcritical crack propagation in rocks have also shown that the chemical interaction between the fluid and rock surface such as ion exchange between the liquid and solid phase, difference in chemical potential could also result in weakening reactions in the crack tip environment.

Apart from drilling studies that have looked at effects of water-based fluids on shale to address well instability problems, little study has been done to evaluate the effects of fracturing fluid additives such as surfactants on the mechanical properties of shale. This study will use characterization of mechanical properties to investigate the use of specific surfactant systems in fracture fluids to enhance fracture initiation and propagation to improve hydraulic fracture performance and overall fluid recovery.

1.2 Literature Review

Several studies have been carried to investigate the effect of surfactants on the strength and material properties in quartz and other geologic materials. According to Dunning et al. (1980), Rehbinder and Westwood proposed theories to explain this effect. In the Rehbinder theory, it was proposed that surfactants cause a reduction in the bonding forces across the developing crack or fracture as a result of adsorption of the surfactant on the surface, hence altering the materials surface energy. The Westwood theory proposed that the zeta potential of fluid environment affects the mobility and nucleation of dislocations at or near the surface of the material, and inhibits or improves the growth of brittle cracks or fractures. Lewis (1976) investigated the rate of

microfracturing in Crab orchard sandstone and in correlation with Westwood's concept, showed that zero zeta potential systems produced maximum brittlization.

Dunning et al. (1980) pointed out that the previous studies did not investigate the crack propagation mechanism, which is key to the process of brittle failure. He carried out tests to study crack propagation in similar environments investigated by the previous studies. His observations suggest that neither of the chemomechanical models of Rehbinder or Westwood could be applied to quartz or silicate geologic materials. Rather, the crack propagation stress is dependent on the availability of absorbable species between the fluid environment and rock surface.

Atkinson (1982) studied the micromechanisms of fracture, subcritical crack propagation in rocks in particular. He identified ways in which chemistry of the phases-both fluid and rock surface could lower the barriers to crack propagation. These ways includes ion exchange between the chemical environment and solid phase, difference in chemical potential between highly stressed atoms of the crack tip and the bulk of solid leading to concentration gradient of vacancies at the tip of the crack, and most importantly stress corrosion which occurs as a result of water, water vapor or other reactive species resulting in weakening reactions in the crack tip environment.

Karfakis and Akram (1993) carried out experiments using dolomitic limestone, Sioux quartizite and Westerly granite, and found that although tensile fracturing is facilitated in aqueous environments, there is no evidence that cracks are more easily initiated and propagated in rocks in a zero zeta potential environment. He also concluded that the microstructure, mineralogy of the rock and chemistry of the solution determines

the extent of activated fracturing. Apart from Karfakis and Akram (1993), most of the previous works investigating the effect of surfactant, have been on crystals of quartz, silica glass, ceramics or sandstone with high quartz content (Dunning et al., 1980).

There have been several studies on shale-fluid interaction to address problems of wellbore stability. The effect of chemical potential and physiochemical interactions between the drilling fluid and shale has been highlighted to be of high relevance to address shale instability. Most authors have developed and proposed improved procedures because of the difficulty in handling shales, preservation of the original moisture content of the shale, preparation of standard-size samples and long fluid circulation time because of low hydraulic permeability of shales. Santos et al. (1997) proposed the use of triaxial cells which reproduces downhole in-situ stresses, and highlighted the importance of using preserved samples which have not lost their original water content especially when the swelling potential is being studied. In his tests, he used preserved shale from the Campos Basin, offshore Brazil and partially dried North Sea reddish shale. De-ionized water was the test fluid used. His results showed that only the dried shale samples presented reactions when in contact with water, while the preserved shale showed no change in deformations, indicating no swelling or contraction.

Corrêa and Nascimento (2005) developed a test for evaluating mechanical properties of reactive shale from a natural outcrop in Calumbi (SE-Brazil) submerged in different fluids using a three-point flexural test submerged in fluid being studied. The shale specimens submerged in air showed the largest mechanical resistance, followed by

specimens submerged in oil, while specimens in water-based fluids (distilled water or aqueous polymeric solutions) showed the lowest mechanical resistance. According to his work, the difference in chemical potential, interactions between the cationic groups and negative sites of the face of the shale influenced the deformation, rigidity. Using thermogravimetry, he also characterized the composition of the shale before and after the test. The specimens submerged in air contained the water content in natural shale; smaller losses were observed in oil, while the aqueous and polymeric solutions showed larger mass losses.

Most of these previous works have evaluated shale-fluid interaction using drilling fluids or water. Since the work aims at investigating shale-fluid interactions during hydraulic fracturing, surfactants are selected as the fluid of contact. Surfactants are one of the key ingredients contained in fracturing fluid. Also with recent development of viscoelastic surfactants (VES) for use as fracturing, fluid instead of polymer gel or slickwater, the results of this work should lend an understanding to the effect of the VES on mechanical properties of shale and overall effect on hydraulic fracture performance.

1.3 Objectives of Research

The overall objective of this research work is to study the chemical interactions between an important ingredient of fracturing fluid- surfactants, and the unconventional rock formation. This will be achieved as follows:

- Shale characterization to understand how the soil interacts with fluid environments as a function of its mineral content, ions available for exchange and its organic matter content.
- Shale-fluid interaction tests to study the effects of the fluid environment on the shale. This will include adsorption experiments, microscopy imaging of induced fractures in selected fluid environment.
- Results from these first two stages will initiate further studies for design of rock deformation experiments to investigate the relative ease of deformation of rock samples in selected chemical fluid environments. These tests will investigate the effect of the fluid environments on the mechanical properties of the shale being studied.

1.4 Outline of Thesis

Chapter II of this study focuses on some theories and fundamentals of shale-fluid interactions. These includes a little section on shale properties and its potential to meet the gas supply challenges in the United States; mineralogy, cation exchange capacity and total organic matter. Chapter II also provides some introduction on hydraulic fracturing fluids, and then narrows down to some details about surfactants which is one of the additives in fracturing fluids. The chapter ends with a look at some concepts in fracture mechanics as factors that can be influenced by fluid interactions.

In Chapter III, the details of the experimental studies for the various tests for shale characterization and shale-fluid interaction is presented. The results from the

experimental studies are analyzed and discussed in Chapter IV, showing possible relationships and effects of aqueous environment on the growth of fractures in the shale samples. Chapter V presents the conclusions of this study, and recommendations for future work.

CHAPTER II

THEORY OF SHALE-FLUID INTERACTIONS

2.1 Shales

When sediments like gravel, sand, mud, peat and accumulations of seashells, accumulate or mineral crystals precipitate from aqueous solutions, they form deposits. When the deposits are consolidated and hardened by the process called lithification, they form sedimentary rocks. Detrital sedimentary rocks are formed from weathered and eroded particles of larger pieces of sedimentary rock. Shale is a detrital sedimentary rock made up of very fine clay-sized particles. Following the grain size classification based on the Wentworth scale, shale is composed of clay-sized particles that are less than 0.0039 mm in diameter. Siltstone is composed of particles that are between 0.0039 and 0.0625 mm in size. When the sedimentary rock is a mixture of clay and silt, geologists call the rock mudstone.

In recent times, “shale gas” is used to refer to natural gas found in hydrocarbon-rich shale formations. It is classified alongside with coal bed methane (CBM) and tight gas as unconventional gas plays and resources, generally because they are lower quality formations with enormous resource concentration and most importantly, they cannot be recovered economically without application of improved stimulation, extraction or recovery technologies. Shales in particular have very low permeability (nanodarcies), which prevents efficient recovery of the natural gas except the formation is fractured. **Fig. 2.1** shows the presence of shale gas approximate locations of producing gas shales

and prospective shales across the lower 48 states. So far, exploration and production in these basins have shown that they have unique challenges. The availability of additional information from drilling and production activities has contributed to the improvement in the development of the resources in these basins.

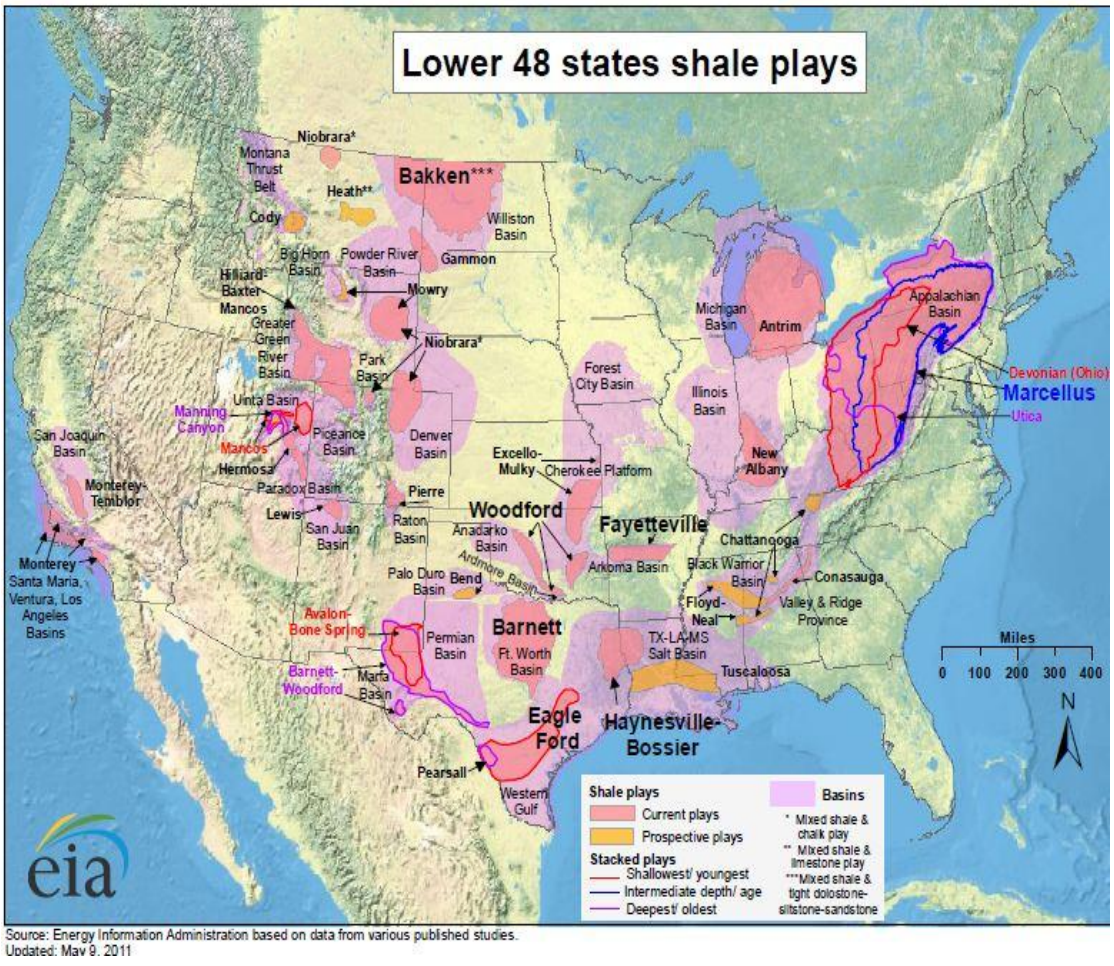

Source: Energy Information Administration based on data from various published studies.
Updated: May 9, 2011

Fig. 2.1—Map of Lower 48 States Shale Plays (as of May 9, 2011). Source U.S. Energy Information Administration.

2.2 Soil Characterization

2.2.1 Mineralogy

Minerals are formed when the necessary elements are present in a rock; hence the chemical composition of a rock determines the minerals present in the rock. The mineralogy of shales is highly variable. Clay is the most common mineral found in shales, other minerals present are quartz, mica, pyrite, and organic matter. Clay is formed from the decomposition of the mineral feldspar. Shale can be red, green or black. The difference in colors is attributed to different minerals in the shale. The knowledge of clay minerals is important because of the negative charge they contribute for cation exchange.

Clay minerals are part of the larger class of silicate minerals called the phyllosilicates. The type of clay formed is determined by the arrangement of the two building sheets- the silica tetrahedron and the aluminum octahedron. The one-to-one (1:1) clays have strong hydrogen bonds between each sheet while the two-to-one (2:1) clays structure have one aluminum octahedron sheet between two tetrahedral sheets. Clay minerals can be classified into three main groups- kaolinite, illite, and smectite. Illite is the most abundant clay mineral, and the main component found in shales and other argillaceous rocks. It has the 2:1 sheet arrangement, and the general formula is (K, H)Al_2(Si, Al)$_4O_{10}(OH)_2$ - xH_2O, where x represents the amount of water the group contains. Kaolinite has the 1:1 sheet arrangement, and a chemical formula of $Al_2Si_2O_5(OH)_4$. It does not absorb water, and hence it has a low shrink-swell capacity. Smectite also has a 2:1 arrangement; hence water molecules can be absorbed between

the sheets resulting in the increase of volume of the minerals. Several minerals including pyrophyllite, talc, vermiculite, sauconite, saponite, nontronite and montmorillonite are classified in the smectite group, and are often referred to as expanding clays. The mineralogy and clay fractions in shales can be determined by methods such as X-Ray diffraction analysis and Fourier transform infrared spectroscopy (FT-IR).

2.2.2 Cation Exchange Capacity

Soil particles containing clay and organic matter have negatively surfaces. These negative charges attract and hold the positively charged ions- cations by electrostatic forces. The measure of the ability of the soil to attract and adsorb exchangeable cations is referred to as the cation exchange capacity (CEC). It is often expressed in in millequivalent per 100 g of dry soil (Meq / 100g). This refers to the amount of cations that can be accommodated on a certain mass of negatively charged surface. According to the Schlumberger oilfield glossary, the CEC can also be expressed in terms of its contribution per unit pore volume, Qv. The CEC of soil largely depends on its mineralogy and amount of organic matter present. Organic matter has a high CEC, hence soil having a high percentage of organic matter have a relatively high CEC. With clay minerals, the 1:1 arrangement have a relatively low CEC because the negative sites yet to be satisfied are only at the edge of the mineral. The clay minerals with the 2:1 arrangement on the other hand have an open interlayer, cations may be present to balance negative charges within the sheet, and hence they have a relatively higher CEC.

2.2.3 Total Organic Carbon

Carbon is formed when plants and animal matter decompose and get leached to the ground. In soils and sediments in both terrestrial and aquatic environments, carbon exists in three basic forms- elemental, inorganic, or organic forms. The total organic carbon is an indirect measure of the presence of organic matter in soils and sediments. The determination of total organic carbon is important in soil characterization because its presence or absence can significantly influence the interaction of the soil with chemicals. According to Schumacher (2002), some of the important characteristics of organic matter include their ability to- form water-soluble and water insoluble complexes with metal ions and hydrous oxides; interact with clay minerals and bind particles together; sorb and desorb both naturally-occurring and anthropogenically-introduced organic compounds; absorb and release plant nutrients; and hold water in the soil environment.

There have been several approaches to measure TOC in soils and sediments. The qualitative approach involves the structural characterization of organic carbon using nuclear magnetic resonance (NMR) or the diffuse reflectance infrared Fourier transform (DRIFT). The quantitative approach either determines the TOC as the difference between the measured total carbon and measure inorganic carbon, or measures the TOC directly after purging the inorganic carbon from the sample.

2.3 Hydraulic Fracturing Treatment

Although the hydraulic fracturing technology has been in use since the early 1940s, the types of fracturing fluids and treatments have evolved over the years. The development was particularly accelerated by the use of the hydraulic fracturing technology along with horizontal drilling to achieve economic gas flow rates and recovery from low permeability reservoirs like shale. The choice of fracturing fluids for hydraulic fracture treatment using water, crosslinked-gel, hybrid, micellar and foam fracture treatments have been influenced by various factors like the reservoir temperature, pressure gradient, Young's modulus of formation, type of upper and lower barrier, desired half-fracture length, height of pay zone and presence of natural fractures. More recently, other factors like cost of treatment and environmental concerns on the effect of hydraulic fracturing treatment on groundwater have received a lot of attention. This has led to legislations that require the disclosure of the fluids used by service companies in the hydraulic fracturing processes. According to these disclosures, these fluid additives are chemicals found in common consumer products like detergents, disinfectants, cosmetics, food and pharmaceuticals.

In the slickwater hydraulic fracture treatment which was first successfully used in the Barnett shale and is being adopted in other shale gas basins. The fracturing fluid consists of 99.5% water and proppant (most often sand), while the additives make up only about 0.5%. These additives include- friction reducer which is used to minimize friction, biocides to prevent organisms from clogging the fissures, scale inhibitors to prevent scale deposits downhole and in surface equipment, and surfactants. While the

initial disposition was to assume that the same treatment should work for all plays or formations, most operators have come to understand the need for reservoir characterization to optimize fracture treatments and improve performance and recovery.

2.4 Surfactants in Hydraulic Fracture Treatment

Surfactants (also known as surface active agents) are organic compounds which are referred to as amphiphilic, because they contain both hydrophobic groups (present in the tails) and hydrophilic groups (present in the heads). Generally, surfactants are used to reduce the tension within a fluid system. In a liquid-gas interface, it reduces the surface tension of water by adsorbing at the interface, while in a liquid-liquid system; it reduces the interfacial tension between oil and water by adsorbing at the liquid-liquid interface. Surfactants are among the fracturing fluid additives used in hydraulic fracturing operations. Laboratory studies backed up by field observations have shown surfactant contribute to increase in gas production by reducing the capillary pressure and changing shale wettability (Zelenev, 2011). Surfactants also act to reduce the surface tension of the fracturing fluids, thereby improving flowback of fracturing fluid from the well after the fracturing process. In addressing questions about the potential harm in using surfactants as additives in fracturing fluids, several articles and sources have documented other common and practical applications of surfactants. These include their use in the manufacture of antiperspirant, deodorants, detergents, fabric softeners, paints, inks, anti-fogging agents, ski wax, foaming agents, laxatives, hair conditioners and agrochemical formulations (wetting agents in herbicides and insecticides).

Surfactants can be classified as either ionic or nonionic depending on if the head contains a charge, and ionic surfactants can be further classified as cationic (positive charge), anionic (negative charge) or zwitterionic (dual charge) depending on the type of charge on the head. When surfactants are added to an aqueous fluid above a certain minimum concentration, the molecules combine to form aggregates known as micelles. The concentration at which they begin to form micelles is referred to as the critical micelle concentration (CMC). When micelles form in water, the hydrophilic head is in contact with the water, while the hydrophobic tails assemble together forming a hydrophobic core that can trap oil droplets or other oleophilic materials. In oil, the aggregates formed are reversed, with the hydrophilic heads trapped in the core while the hydrophobic tails are in contact with oil.

With some surfactants, when added to an aqueous fluid in which certain salts are present within a particular concentration range, the micelles formed have rod-like structures which become entangled. These micelles exhibit viscoelastic properties-increased viscosity and elasticity, and hence are called viscoelastic surfactants (VES). The property exhibited by VES has made them attractive for hydraulic fracturing, because the increased viscosity of the fracture fluid improves effective proppant transport.

2.5 Adsorption of Surfactants

Surfactants have the ability to alter the properties of interfaces through adsorption (Shchukin et al., 2001). In a solid-liquid interface, adsorption of surfactant

molecules from bulk solution phase to the interface can occur depending on factors like the natures of the surfactant and fluid surface, surfactant concentration, pH and temperature. According to Zhang and Somasundaran (2006), the mechanism governing adsorption could be a combination of driving forces such as the electrostatic interaction, the chemical interaction, the lateral chain–chain associative interaction, the hydrogen bonding and desolvation of the adsorbate species.

Electrostatic interactions play a governing role in systems where both the surfactants and the solid particles are charged. If the ionic surfactant and solid particles are oppositely charged, the rate of adsorption is faster compared to if they were similarly charged. When there is covalent bonding between the surfactant and mineral surface, adsorption is seen to occur by chemical interaction. In the lateral chain–chain associative interaction mechanism, the free energy from the transfer of hydrocarbon chains from the aqueous environment into the hydrophobic interior of the aggregates formed at concentrations above a threshold serve as the driving force for adsorption. Hydrogen bonding between the surfactant and the solid surface occur in systems where the surfactant contains functional groups such as hydroxyl, phenolic, carboxylic and amine groups. Adsorption takes place as a result of this mechanism if the hydrogen bond between the functional groups and mineral surfaces is stronger than the bond formed between the mineral and interfacial water molecules.

There is still a lot of learning going on in the behavior of surfactants in the soil due to the difficulty of establishing the adsorption-desorption mechanism, and the complex molecular structure of surfactants. According to Rodríguez-Cruz et al. (2005),

while some authors have reported the correlation between adsorption and the amount of organic matter present in soils, other authors have reported the correlation between adsorption and clay content of the soil. Some authors (Deng et al., 2006a, 2006b; Rodríguez-Cruz et al., 2005; Sánchez-Martín et al., 2008; Zhang and Somasundaran, 2006) have studied the adsorption of surfactants and polyacrylamides on clay minerals. Their studies have shown the importance of physiochemical and mineralogy of clay fraction in understanding surfactant behavior in applications such as solubilization, remediation of soils by removal of toxic contaminants and further more design of novel organo-clay composites to immobilize dissolved contaminants. These studies also inform the need for such understanding of interactions between surfactants used in fracturing fluids and their interaction with the formation.

2.6 Rock Mechanics in Hydraulic Fracturing

Rock mechanics has been of great value in developing hydraulic fracturing theories. The study of rock deformation and failure and concepts of fracture propagation have particularly been applied to understanding the factors influencing hydraulic fracture initiation and propagation.

2.6.1 Deformation and Failure of Rock- Compressive Stress

The most common method of studying the mechanical properties of rocks is by axial compression of a cylinder with length to diameter ratio of 2 or 3. If the lateral surface of the rock is traction-free, the configuration is referred to as uniaxial compression or unconfined compression. The axial stress, σ is the controlled,

independent variable, while the axial strain, ε is the dependent variable. The state of stress in the rock is $\sigma_1 > 0$ and $\sigma_2 = \sigma_3 = 0$, where σ_1, σ_2, σ_3 are the principal stresses. The uniaxial compression test is used to determine the Young's modulus, *E*, which is estimated as $E = \sigma / \varepsilon$. The stress at which the rock fails is known as the unconfined, or uniaxial compressive strength of the rock, C_o.

If the lateral surface of the rock has traction applied, the configuration is referred to as triaxial or confined compression. In this case, the state of stress in the rock is $\sigma_1 > \sigma_2 = \sigma_3 > 0$. Depending on the configuration of a triaxial compression experiment, the hydrostatic pressure may act in all three directions or only over the two lateral surfaces of the rock. The equal lateral stresses are referred to as the confining stress, while the third principal stress is referred to as the axial stress. The difference between the axial and confining pressure is referred to as the effective stress, $\sigma_1 - \sigma_3$.

The traditional triaxial tests are not capable of investigating the effects of the intermediate principal stress; hence conducting test with the three principal stresses having different and independent values is desirable- is $\sigma_1 \geq \sigma_2 \geq \sigma_3 \geq 0$. This is sometimes referred to as the polyaxial or true-triaxial test. The design of this tests use rectangular specimens instead of the conventional cylindrical samples used in uniaxial and traditional triaxial tests (Jaeger et al., 2007).

2.6.2 Failure Criterion

The process of rock failure is complex because it is difficult to understand the precise details of crack initiation and propagation, or the total structural breakdown as

microcracks propagate and coalesce. The mostly widely used failure criterion is the Mohr-Coulomb criterion. Based on his experimental investigations into friction, Coulomb assumed that failure in a rock occurs along a plane due to the shear stress acting along that plane. The Mohr-Coulomb criterion therefore expresses the relation between the shear stress, τ and the normal stress, σ_n at failure.

$$\tau = C + \mu \sigma_n. \quad \text{..... (2.1)}$$

The parameter denoted by C is the cohesion while the parameter denoted by μ is the coefficient of internal friction. Mohr's circles are drawn using the failure stresses obtained at different confining pressures in a multistage triaxial test. The common tangent to these circles gives the failure envelope as shown in **Fig. 2.2**. The slope of the common tangent gives the coefficient of internal friction and its intercept with the τ-axis is the measure of cohesion. The angle which this tangent makes with the σ_n-axis is known as the angle of internal friction, denoted as φ.

$$\varphi = \tan^{-1} \mu. \quad \text{..... (2.2)}$$

The Mohr-Coulomb criterion is most useful and applicable at high confining pressures when the material fails through development of shear planes. It cannot be applied directly at lower confining pressures, and in the uniaxial case, where failure occurs by gradual increase in the density of microcracks sub-parallel to the major principal stress (Harrison and Hudson, 2000).

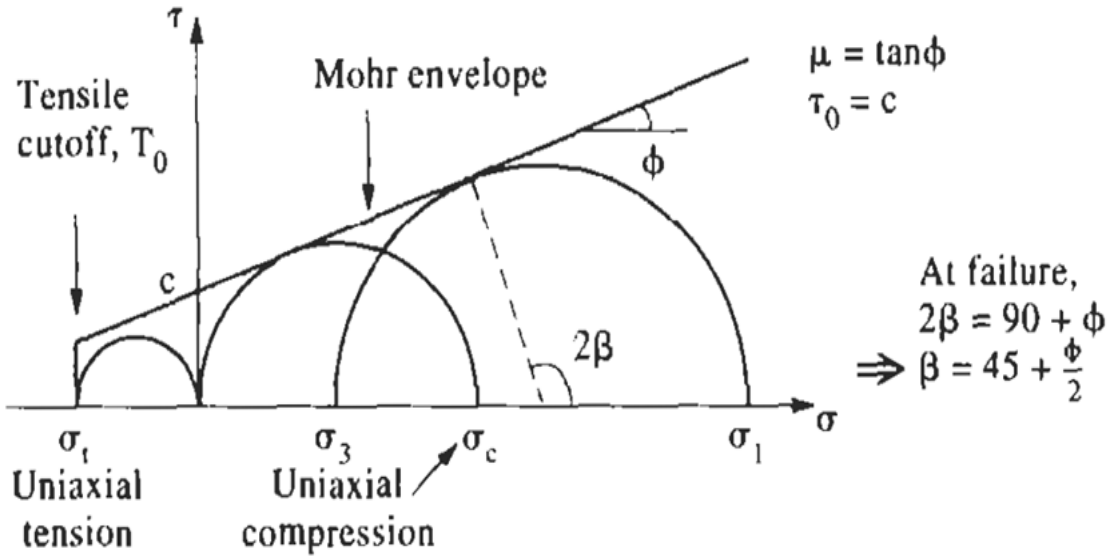

Fig. 2.2—The Mohr-Coulomb Failure Criterion (Harrison and Hudson, 2000)

2.6.3 Deformation and Failure of Rock- Tensile Stress

The tensile strength is the maximum strength it can resist while being pulled apart in the axial direction without yielding or fracture. Since a direct-pull uniaxial test will be difficult to apply to rocks, an indirect test is employed to determine tensile strength. The Brazilian test is a diametric compression test where a disc of the test material is loaded across a diameter.

2.7 Fracture Initiation and Propagation

The concept of linear elastic fracture mechanics (LEFM) can be employed to measure and characterize the resistance of crack growth of shale rock in aqueous

environments. The stress intensity factor, K_I is a measure of the resistance to fracture. It indicates the state or strength of the stress near the tip of a crack.

$$K_I = Y\sigma a^{1/2}. \quad \text{..... (2.3)}$$

where Y is a constant depending on geometry of loading,

σ is the uniform applied stress, and

a is the characteristic crack length.

When the stress intensity factor at the crack tip is above the critical value known as the fracture toughness of the material, K_{IC}, the crack will propagate; below this value the crack will not propagate. Fracture toughness has been of relevance in drilling design to prevent undesired fracturing of the formation. This understanding can be used in the reverse stimulation operations in which case the objective is to initiate and propagate a fracture.

There are three basic modes of crack tip deformation, commonly identified as Mode I, Mode II, and Mode III (shown in **Fig. 2.3**). When the forces are perpendicular to the crack, with the forces pulling the crack open in the top and bottom directions, this is referred to as Mode I (opening mode). When the forces are parallel to the rock, pulling (actually sliding) the top and bottom halves along its original plane but in opposite directions, this is referred to as Mode II (shearing mode). In Mode III (tearing mode), the forces are perpendicular to the crack with the forces pulling in the left and right directions. The material separates and slides along itself, but moves out of its original plane. Mode I is considered to be the weakest mode. Here, the cracks propagate parallel

to their own plane. This plane is the most stable orientation for crack propagation because it experiences maximum tensile stress.

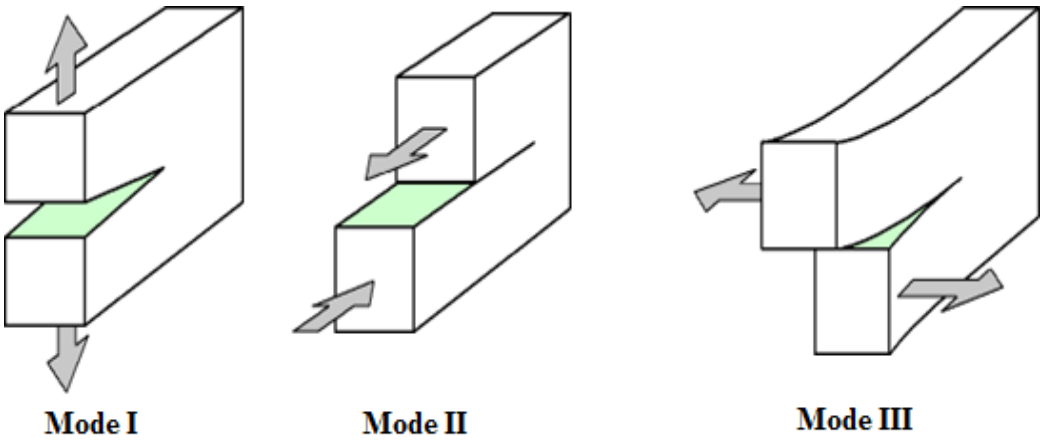

Fig.2.3—Fracture Mode (http://www.efunda.com/formulae/solid_mechanics/fracture_mechanics/fm_lefm_modes.cfm)

2.8 Mechanisms of Subcritical Crack Growth

Atkinson (1987) in his work and compilation of similar works has presented a detailed broad overview of subcritical crack growth in rock, some aspects of which are summarized in this section. Fracture mechanics is important in study of subcritical cracking because the crack tip stresses causing the crack growth are directly proportional to the stress intensity factor, K_I. Most often, the critical stress intensity factor approach has been used to predict crack propagation in metals, ceramics and glasses. However, this classical approach breaks down if high temperatures or reactive environments are

present. With materials like oxides and silicates, cracks can propagate at significant rates where the K_I is significantly lesser than K_{IC}. This is referred to as subcritical crack propagation Subcritical crack propagation can occur due to competing mechanisms such as stress corrosion, dissolution, diffusion, ion-exchange and microplasticity. The type of mechanisms prevalent depends largely on the materials being investigated- silicates, quartz, or carbonates.

Stress corrosion crack growth occurs when cracking is influenced by the presence of chemical environments, such as water, and weakens the strained bonds at crack tips. For silicate glasses, the strained Si−O bonds react more readily with the chemical environment than the unstrained bonds. With water, the silicate minerals undergo corrosion according to Equation (2.4), while in basic environments; they undergo corrosion according to Equation (2.5).

$$H{-}0{-}H + [\equiv Si{-}0{-}Si\equiv] \leftrightarrows \equiv Si{-}OH \cdot HO{-}Si\equiv \leftrightarrows 2[\equiv Si{-}OH]. \quad \text{..... (2.4)}$$

$$0H^{-} + [\equiv Si{-}0{-}Si\equiv] \leftrightarrows \equiv Si{-}O^{-} + \equiv Si{-}OH. \quad \text{..... (2.5)}$$

These reaction equations are proposed based on results of experimental work using glass. With quartz, simple or even more complex silicates, more possible reactions may accompany the stress corrosion cracking. Stress corrosion involves the formation and propagation of a cloud of microcracks in the process zone at a macrocrack tip. Microcracks are planar discontinuities with dimensions of the order of one to several grain diameters (about 100 to 1000 microns).

Diffusional mass transport can also contribute to subcritical crack growth. Materials that exhibit intergranular cavitation that are perhaps initiated by grain

boundary sliding and nucleated at grain boundary impurity segregations will be more susceptible to this form of mechanism. Possible diffusion paths that have been identified include lattice or bulk diffusion, surface diffusion, vapor phase transport and grain boundary diffusion. The occurrence of stress directed diffusion of chemical impurities to crack tips facilitates weakening chemical reactions that allow crack growth. The solubility of minerals and their dissolution rate also play a role in controlling the growth of crack. Some factors such as temperature, solution density, and pH can influence the solubility of the minerals. Calcite is quite soluble in water at room temperature and is much more soluble than quartz. Equations 2.6 and 2.7 show the dissolution reactions of carbonates and quartz respectively.

$$C0_2 + H_20 + CaC0_3 \leftrightarrows Ca^{2+} + 2HCO3^{-}. \quad (2.6)$$

$$Si0_2 + 2H_2O \leftrightarrows Si0_2 \cdot 2H20_{aq}. \quad (2.7)$$

Crack propagation can occur due to lateral strains resulting from ion exchange between the chemical environment and the solid phase. The importance of the contribution of ion exchange reactions to subcritical crack propagation depends on the ease of the modification of the solution at the crack tip by diffusional exchange with the bulk external environment. The growth pattern is controlled by the crack velocity, the rate of reaction between the aqueous environment and the material of the crack tip, and the chemistry of the solid. At high crack velocities, the crack growth is controlled by the chemical composition of the new crack surfaces since the creation of new sources of reactive ions in fresh crack surfaces occurs faster than the transport of chemical species from the bulk fluid to the crack tip environment. At low crack velocities, the crack tip

environment is open to modification by the external environment through diffusion of chemical species along the crack. Hence, the crack growth is controlled by the chemical differences between the crack tip fluid and the bulk fluid.

In crystalline materials, catastrophic fracture can be controlled by pre-existing cracks, cracks generated through microplasticity, cracks generated through plasticity or cleavage and intergranular fracture. Microplasticity can give rise to subcritical crack growth. In the stress field, when the local conditions for slip or twinning are satisfied, a crack will propagate once formed and fracture occurs at the stress for the onset of microplasticity. Microcracks of various orientations and positions will be nucleated and some of these grain boundary and cleavage microcracks will eventually link up to allow macrocrack extension. The process will be locally episodic, involving rapid crack extension alternating with periods of relative crack stability. However, macroscopically, the process appears as quasi static subcritical crack growth. This type of crack growth is influenced by temperatures, low strain rates and the chemical environment.

CHAPTER III

EXPERIMENTAL STUDIES

The experimental work consists mainly of the shale characterization and shale-fluid interaction tests. While the characterization tests are aimed at determining the composition and some properties of the shale, the shale- fluid interaction tests study the effects of the fluid environment on the shale. **Fig. 3.1** presents a pictorial view of the workflow for this study.

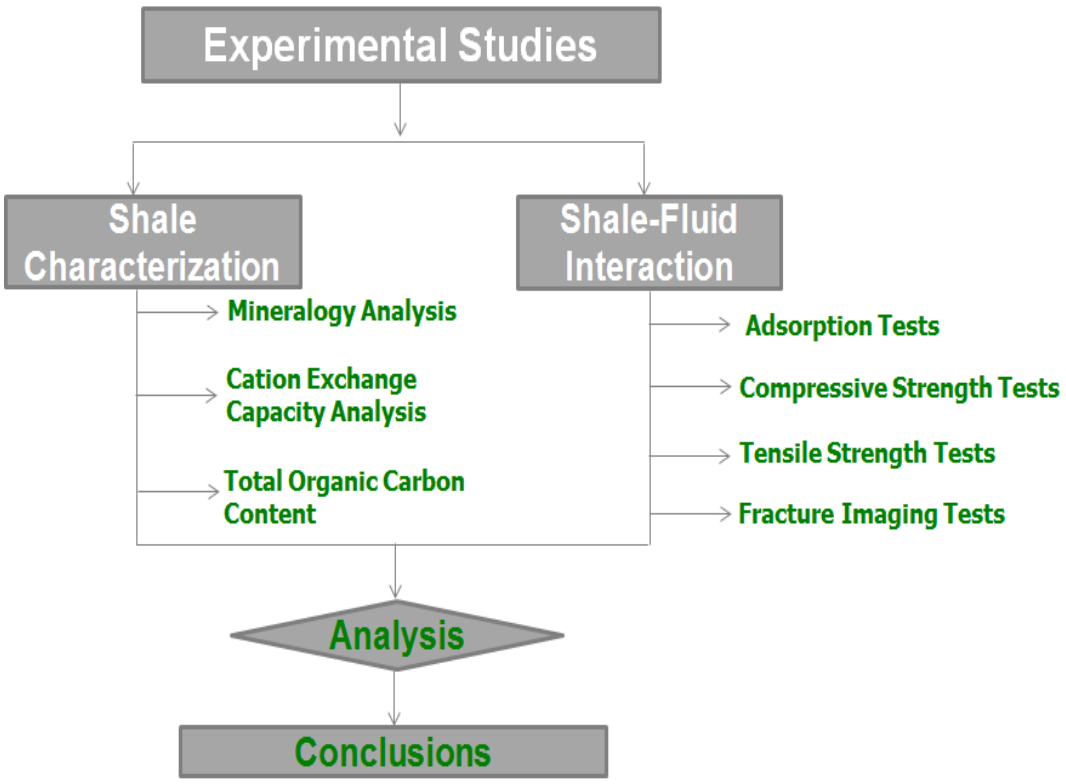

Fig. 3.1—Workflow for Experimental Studies

The shale samples used for this study were from the Mancos shale play. The commercial samples were purchased from the Hard rock division of Kocurek industries. The Mancos shale which was mined out from south of Salt Lake City, Utah, at depths of about 20 – 60 ft. Cylindrical samples of 1 inch diameter by 2 inch length were cored from a single block. **Table 3.1** shows the properties of the Mancos shale.

Table 3.1—Showing Some Properties of the Mancos Shale Rock Samples

Porosity, %	3.7 - 7.9
Permeability, md	< 0.001
Bulk Density, g/cm^3	2.52 - 2.58
Grain Density, g/cm^3	2.64 - 2.70
Uniaxial Compressive Strength, psi	6300 - 9800
Young's Modulus, 10^6 psi	0.9 - 2.1
Poisson's Ratio	0.36 - 0.39

The shale sample characterization tests carried out are the following:

- Mineralogy analysis
- Cation exchange capacity analysis
- Determination of organic carbon

These tests are important to understand how the soil interacts with fluid environments as a function of its mineral content, ions available for exchange and its organic matter content.

3.1 Determination of Mineralogy

The qualitative mineralogy analysis of the Mancos shale was done using both the X-ray diffraction (XRD) and Fourier transform infrared spectroscopy (FT-IR). The shale samples were broken into smaller pieces using a mallet, ground into fine particles using a mortar and pestle and sieved through a 200 mesh sieve. The XRD analysis was carried out in the X-ray Diffraction Laboratory in the department of Chemistry using the Bruker D8 Advance instrument. The procedure for this analysis is summarized as follows. The sample was placed in the sample holder of a two circle goniometer, enclosed in a radiation safety enclosure. The X-ray source was a 2.2kW Cu X-ray tube, maintained at an operating current of 40 kV and 40 mA. The X-ray optics was the standard Bragg-Brentano para-focusing mode with the X-ray diverging from a DS slit (1mm) at the tube to strike the sample and then converging at a position sensitive X-ray Detector (Lynx-Eye, Bruker-AXS). The two-circle 250mm diameter goniometer was computer controlled with independent stepper motors and optical encoders for the θ and 2θ circles with the smallest angular step size of 0.0001^{o} 2θ. The software suit for data collection and evaluation is windows based. Data collection is automated COMMANDER program by employing a DQL file. Data is analyzed by the program EVA.

The FT-IR analysis was carried out in the Soil/Clay Mineralogy Laboratory it the department of soil and crop sciences at Texas A&M University using the PerkinEmer Spectrum 100 Spectrophotometer. Two sets of analysis were carried out using the Universal Attenuated Total Reflectance accessory (UATR) and the Diffuse Reflectance sampling accessory (DRIFT). The UATR technique involves placing a sample on top of a crystal with a high refractive index. An infrared beam from the instrument is passed into the accessory and up into the crystal. This is then reflected internally in the crystal, and back towards the detector which is housed in the instrument. For the analysis using the DRIFT accessory, there are two sampling positions- the background and the sample. As the beam enters the DRIFT, it is focused by an ellipsoid mirror onto the sample. The mirror collects the reflected beam and directs it on to the detector within the instrument.

The bulk clay fraction analysis was carried out at the Geology and Mineralogy Laboratory of Ellington & Associates, Inc. using the Bruker D4 unit and the quantitative analysis of the minerals was done using BGMN, a new fundamental parameter-based Rietveld program. The XRD definition of the clay mineral groups was based on the reflection of samples in air-dry and ethylene glycol-saturated states.

3.2 Determination of Cation Exchange Capacity (CEC)

The CEC analysis was determined using the pH 7.0 ammonium acetate procedure of Chapman (1965). The shale samples were broken into smaller pieces using a mallet, ground into fine particles (less than 2mm size). The equipment, reagents,

procedure and calculation used by the Texas A&M Soil Characterization laboratory are described as follows.

Equipment:

- 24 place, mechanical extractor
- 24 each, 60 cc plastic (polypropylene) syringes, sample tubes, and reservoirs.

Reagents:

- Sodium Acetate (NaOAc) 1 N, pH 8.2. Mix 136.08 g of NaOAc in deionized H_2O for each liter of solution desired. Allow time for solution to cool to room temperature. Adjust pH to 8.2 with sodium hydroxide (NaOH) or acetic Acid (CH_3COOH) as needed.
- Ethanol, 95%.
- Ammonium Acetate (NH_4OAc), 1 N, pH 7.0. Mix 68 ml of reagent grade ammonium hydroxide (NH_4OH) and 57 ml of reagent grade acetic acid (CH_3COOH) per liter of solution desired. Bring to volume with deionized water, and cool to room temperature. Adjust pH to 7.0 with NH_4OH or CH_3COOH as needed.

Procedure:

1. Pack approximately .5 g filter pulp into each sample tube.
2. Weigh 2.50 g, < 2 mm air dry soil and transfer into sample tube. Install tubes in the upper disc of the extractor.
3. Install Na syringes.

4. Using a squeeze bottle containing pH 8.2 NaOAc, wash down the inside of the sample tubes.
5. Add NaOAc to the 20 ml mark of each sample tube.
6. Extract rapidly until the depth above each sample pad is about 3 to 5 ml.
7. Install Na reservoirs.
8. Add about 40 ml of NaOAc to each reservoir.
9. Extract for 2 hours; remove reservoirs.
10. Discard NaOAc extract.
11. Return extractor to starting position.
12. Reattach Na syringes to sample tubes.
13. Rinse wall of sample tube with ethanol and fill to 20 ml mark.
14. Extract rapidly until the depth of ethanol above each sample pad is 3 to 5 ml.
15. Install NH_4 reservoirs and fill to 40 ml mark with ethanol.
16. Extract for 45 min.
17. Remove reservoir and syringe and discard ethanol extracts.
18. Return extractor to starting position and add about 5 ml of ethanol to the sample. Reattach the NH_4 reservoirs.
19. Add about 40 ml of ethanol to NH_4 reservoirs and extract for 45 minutes.
20. Remove reservoirs, discard ethanol, and return extractor to starting position.
21. Install numbered syringes.
22. Add pH 7.0 NH_4OAc to 20 ml mark.
23. Extract rapidly until depth of NH_4OAc above sample pad is about 3 to 5 ml.

24. Install NH_4 reservoirs and fill to 40 ml mark with NH_4OAc.
25. Extract for 2 hours.
26. Remove syringes. Transfer extract to a tarred bottle and record weight of extract.
27. Determine concentration of Na in the extract by flame emission on the atomic absorption spectrometer. Use standards with the proper matrix (NH_4OAc) at 0, 5, 20, 40ppm.

Calculations:

CEC as (Meq/100g) = (extract wt.) (mg/1 Na) (dilution)/ (sample wt.) (230)

3.3 Determination of Total Organic Carbon (TOC)

The TOC content was determined using the quantitative approach where the difference between the total carbon content and inorganic carbon content measured. The Chittick's procedure was used in the determination of total carbonate content (inorganic carbon). The test is used to determine the amount of calcite, dolomite and calcium carbonate equivalent present in the sample. The apparatus, reagents, procedure and calculation used by the Texas A&M Soil Characterization laboratory are described as follows.

Apparatus:

Chittick apparatus as shown in **Fig. 3.2**.

Reagents:

Hydrochloric acid (HCl), 6 N, with 3% ferrous chloride ($FeCl_2$). Dilute concentrated HCl 1:1 with water and allow to cool. Determine approximate amount of acid to be used

during the day's determinations and weigh appropriate amount of $FeCl_2$ (3 g per 100 ml) into a beaker. Add acid and stir until $FeCl_2$ dissolves. This solution deteriorates. Do not mix in advance of the determination.

Procedure:

1. Mill grind 15 to 20 g of < 2mm samples for .20 minutes in the large mill.
2. Weigh appropriate amount of mill ground soil (**Table 3.2**) to the nearest milligram into a decomposition flask.

Table 3.2—Showing Sample Weight as Determined by Fizz Test

Effervescence Class	**Sample Weight (g)**
0	Do not run
1	3
2	2
3	1
3+ or Carbonate Rock	0.5

3. Place a stir bar in the flask and add 2 drops of amyl alcohol.
4. Fill the burette tip with HCl-$FeCl_2$ solution and install the sample flask in the system. Fill the burette to the 5 ml mark with HCl- $FeCl_2$.

5. Open the 3-way stopcock to the atmosphere and adjust the liquid level in the measuring burette to +20 ml (above 0) with the leveling bulb.
6. Close the system to the atmosphere with the 3-way stopcock (180^o rotation) and lower the leveling bulb about 5 ml.
7. Simultaneously begin to add HCl-$FeCl_2$ solution to the sample and begin lowering the leveling bulb. The leveling bulb should be kept 1 to 2 cm below the liquid level in the measuring burette.
8. After the sample is moistened, turn on the magnetic stirrer at a slow stirring rate.
9. Close stopcock after 20 ml of acid has been dispensed (25 ml mark).
10. After 30 sec. from the time you open the stopcock, equalize liquid levels in the leveling bulb and the measuring burette and read and record the volume of CO_2 that has been evolved. Also record the temperature and barometric pressure.
11. Turn off magnetic stirrers except for 15 to 30 sec stirring period every 5 to 10 min. Maintain liquid level in leveling bulb 1 to 2 cm below that in the measuring burette.
12. After 30 min., repeat measurements as in step 10, if CO_2 is still, evolving at the end of 30 min., do not make this measurement until gas evolution has stopped.

Calculations:

The calculations involved here require that CO_2 density and air density be estimated from temperature and barometric pressure. The equations given here are based on multiple regression analysis of values from standard tables and van der Waal's Equation of State against temperature (T) and barometric pressure (P).

Air density = $0.00977 + 0.00171\ P - 0.00000609\ TP + [0.0000130\ T^2]$

CO_2 density = 0.0208 + 0.00262 P - 0.0000093 TP + [0.0000186 T^2]

Air Mass (g) = (355.0*)(Air density at 30 sec.)

CO_2 Mass 1 = (30 sec. volume)(CO_2 density at 30 sec.)(1000)

Air volume = (Air mass)(Air density at 30 min.)

CO_2 Mass 2 = (30 min. reading + 355.0 - Air volume)(CO_2 density at 30 min.)(1000)

CO_2 from dolomite = (CO_2 Mass 2 - CO_2 Mass 1)($0.96^{\#}$)

CO_2 from calcite = CO_2 Mass 2 - CO_2 from dolomite

Calcite (%) = (CO_2 from calcite X 100)/(0.4401) X (sample wt.)

Dolomite (%) = (CO_2 from dolomite X 100 X 1.05**)/(0.4773 X sample wt.)

$CaCO_3$ equivalent (%) = % calcite + (1.085 X % dolomite)

* = *approximate volume of air in the system.*

$^{\#}$ = *4% of the dolomite is assumed to react within the first 30 sec.*

** = *5% of the dolomite is assumed to remain unreacted after 30 min.*

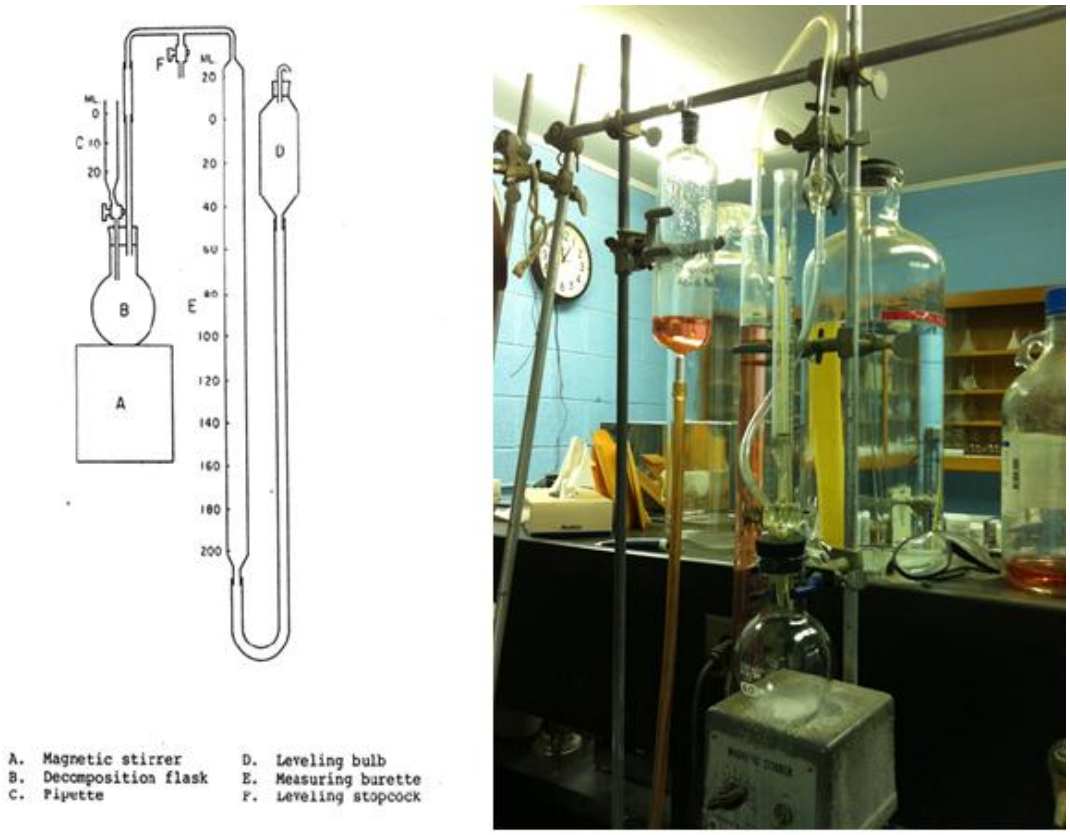

Fig. 3.2—Chittick Apparatus

The total carbon test is essentially a combustion technique in which the sample is allowed to burn in a combustion furnace in the presence of a stream of oxygen. The apparatus, procedure and calculation used for the total carbon test by the Texas A&M Soil Characterization laboratory are described as follows.

Apparatus:

Tube furnace and scrubbing train as shown in **Fig. 3.3**.

Procedure:

1. Preheat combustion furnace to 950^{o}C. Begin sweeping system with oxygen at a rate of approximately 100 cm^{3} per minute.
2. Determine initial weight of two adsorption bulbs.
3. Connect the inlet of one of the bulbs to the flow tube and immediately open the stopcock.
4. Insert sample of known weight into the center of the furnace (mark on rod) and immediately reinsert the stopper to begin flow.
5. Ignite the sample for 10 minutes.
6. At the end of the ignition period, close the stopcock on the adsorption bulb and immediately disconnect the bulb from the flow. Remove the ignited sample from the furnace and allow oxygen to sweep the system while the second bulb is readied.
7. Weigh the bulb and record as final weight.
8. Repeat steps 3 through 7 for subsequent samples.

Calculation:

% carbon = (final bulb weight – initial bulb weight) (27.3) / sample weight

The total organic content is then calculated as the resulting difference between the total carbon and the total inorganic carbon determined previously from the Chittick's test.

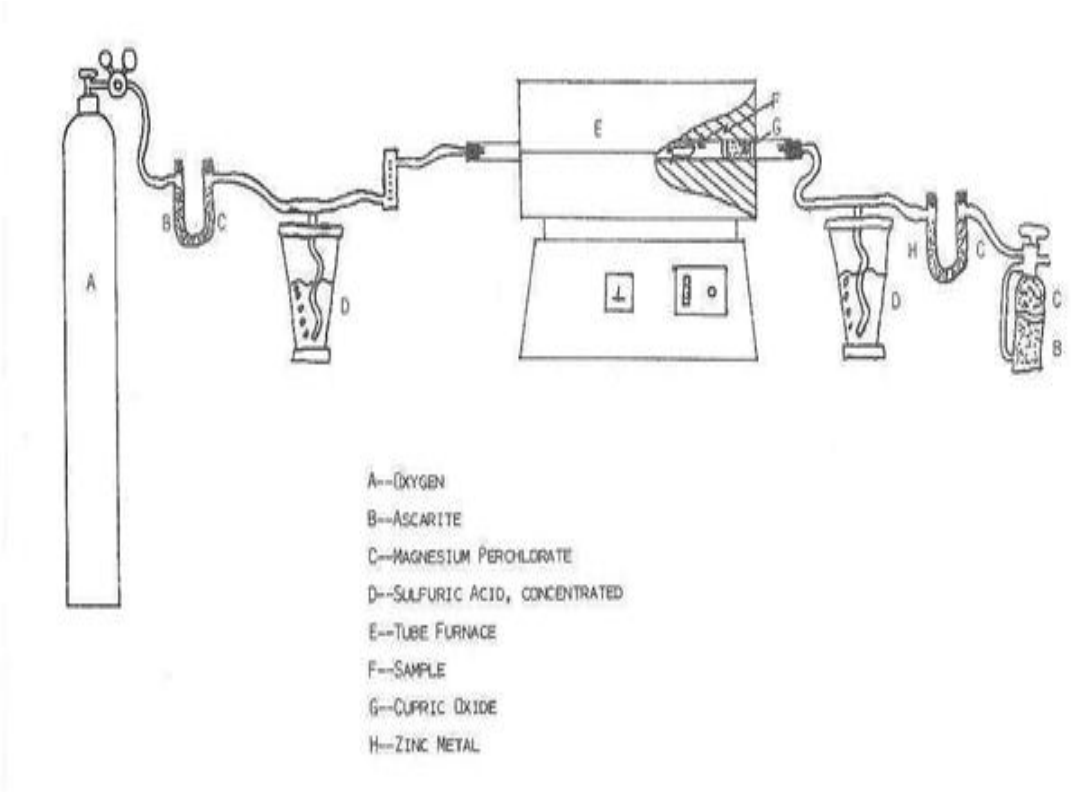

Fig. 3.3—Carbon Train Apparatus

3.4 Shale-Fluid Interaction Tests

Mass transfer processes likely to be important in studying shale-fluid chemical interactions include ion exchange, mineral dissolution and precipitation, adsorption and desorption. It is desired to investigate the chemical alterations of the strength of the shale in the presence of surfactant solutions.

3.4.1 Selected Fluid Environment

The cationic surfactant used in this study is dodecyltrimethylammonium bromide (DTAB). The structure is shown in **Fig. 3.4**. The 88% technical grade chemical was

supplied by Acros organics. DTAB is a quaternary ammonium compound (QAC) in which organic radicals have been substituted for all four hydrogen atoms of the original ammonium cation. This central nitrogen atom which is joined to four organic radicals forms the hydrophobic polar head group while the other end of the long chain is the hydrophilic tail. The negatively charged bromine ion acts as the counter ion. The adsorption of QACs with chain lengths greater than a critical value- eight carbons- such as DTAB takes place via cationic exchange and hydrophobic bonding. It has a critical micellization concentration (CMC) of 1.6 x 10^{-2} mol.dm^{-3} at 25^{o}C (Ananda et al., 1991; Huang et al., 1989).

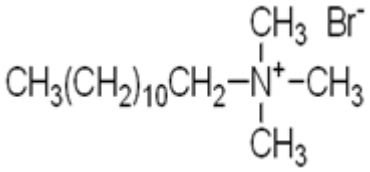

Fig. 3.4—Molecular Structure of Dodecyltrimethylammonium Bromide

Sodium dodecylbenzenesulfonate (SDBS) is the anionic surfactant used in this study. The structure is shown in **Fig. 3.5** The 98% grade chemical was supplied by Sigma-Aldrich.

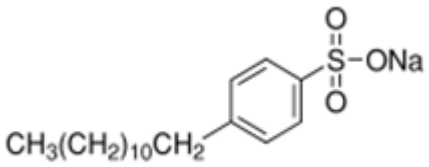

Fig. 3.5—Molecular Structure of Sodium Dodecylbenzenesulfonate

Anionic surfactants are organic compounds which produce large anions containing hydrocarbon chain when dissociated in water (Shchukin et al., 2001). SDBS is an alkylbenzenesulfonate which is usually synthesized by the alkylation of benzene with chloroalkanes or alkenes. It has a critical micellization concentration (CMC) of 1.6 x 10^{-3} mol.dm^{-3} at 25^{o}C (Huang et al., 1989). Some of the properties of DTAB and SDBS are listed in **Table 3.3**.

Table 3.3—Properties of Cationic and Anionic Surfactant

	DTAB	**SDBS**
Molecular Formula	$C_{15}H_{34}BrN$	$C_{18}H_{29}NaO_3S$
Molecular Weight, g/mol	308.34	348.48
Melting Point	246°C	300°C

3.5 Adsorption Test

The evaluation of adsorption is often done by the surface tension differential measure of fluids in contact with the adsorbent (Kaufman et al., 2008). The adsorptive behavior of water, cationic and anionic surfactant with the shale sample was determined by batch equilibrium adsorption process. The initial surface tension of all the solutions- water, $2.85x10^{-4}$ $mol.dm^{-3}$ cationic surfactant- DTAB and $2.81x10^{-4}$ $mol.dm^{-3}$ anionic surfactant- SDBS; were measured using the Wilhemy plate and recorded.

Some aggregates of Mancos shale are ground, air-dried and sieved through 70-mesh (< 0.211mm). 4 g of ground shale is added to 25ml of each solution in a 30ml vial. The systems were shaken and allowed to equilibrate for 24 hours to allow enough time for adsorption take place. After adsorption, the system was left for enough time to allow separation and settling of the shale particles. Surfactant aliquots were taken from each system and the final surface tension was measured.

The resulting difference of the surface tension values before and after adsorption (initial and after equilibrium) was used to determine the amount of surfactant adsorbed. **Fig. 3.6** shows the system of mixtures for solutions for the cationic surfactant, water and anionic surfactant respectively with equal amount of ground shale present. The surface tension experiments are carried in triplicates using the Wilhemy plate (**Fig. 3.7**) in the Advanced Characterization of Infrastructure Materials (ACIM) laboratory in the Civil Engineering department.

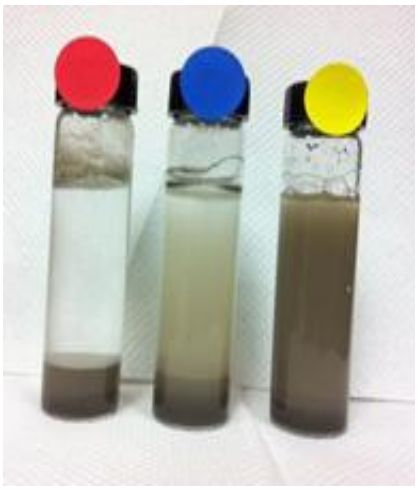

Fig. 3.6—System Mixture of Shale-DTAB, Shale-Water and Shale-SDBS (from left to right)

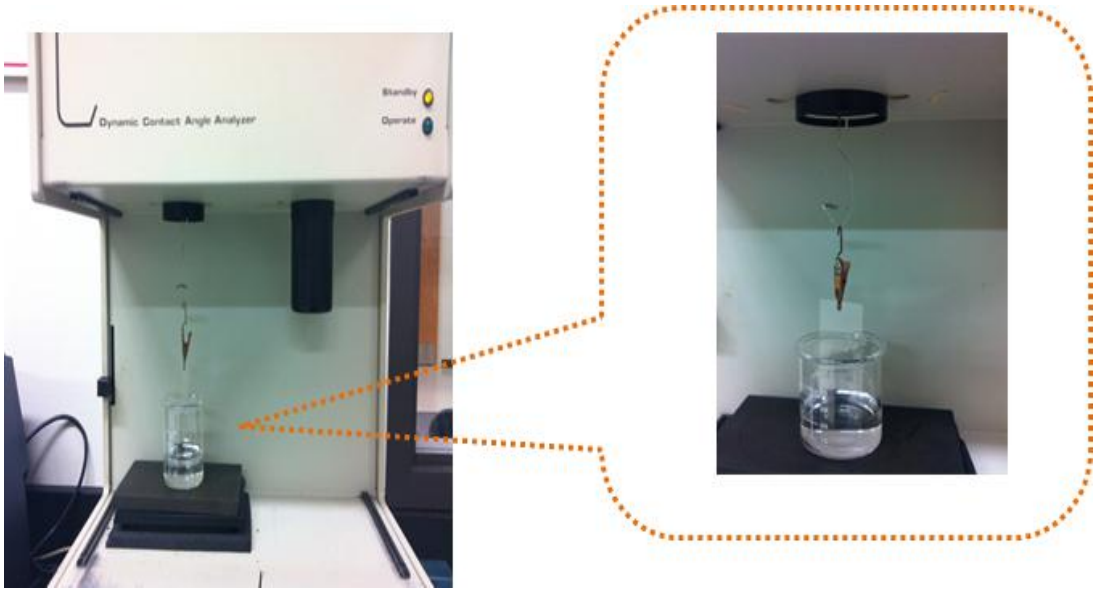

Fig. 3.7—Wilhemy Plate Used for Measuring Surface Tension

3.6 Unconfined Compression Test

Cylindrical shale cores of 1-inch diameter by 2 inch length (with the two-inch length cut parallel to the bedding plane as shown in **Fig. 3.8**) are tested in different environments to determine the relative unconfined compression strength. The GCTS digital point load test system is used along with unconfined compression platens for these tests. The experimental setup is shown in **Fig. 3.9**. The rock sample is loaded until a fracture occurs. The maximum load for failure of each sample is recorded and the corresponding unconfined compressive strength is computed. This test is carried out for dry samples, samples soaked in water for 4 hours, samples soaked in 2.85×10^{-3} $mol.dm^{-3}$ cationic surfactant- DTAB and samples soaked in 2.81×10^{-3} $mol.dm^{-3}$ anionic surfactant- SDBS for 4 hours. Owing to the observed variation of each specimen, and heterogeneity for shale samples as reported in several literatures, about 5 samples were tested for each fluid environment. The mean values and standard deviation were also computed and reported.

Fig. 3.8—Cylindrical Mancos Shale Core

Fig. 3.9—Experimental Setup for Unconfined Compression Test

3.7 Brazilian Test

Disc-shaped cores of 2 inch diameter by 1 inch width (as shown in **Fig. 3.10**) are tested in different environments to determine the indirect tensile strength. The top and bottom loading jaws for the Brazilian test are fitted into the GCTS compression frame. The experimental setup for this test is shown in **Fig. 3.11**. The rock sample is loaded in compression across its diameter and loaded until a fracture occurs. The maximum load for failure of each sample is recorded and the corresponding tensile strength is computed. This test is carried out for dry samples, samples soaked in water for 4 hours, samples soaked in 2.85×10^{-3} mol.dm^{-3} cationic surfactant- DTAB and samples soaked in 2.81×10^{-3} mol.dm^{-3} anionic surfactant- SDBS for 4 hours. Owing to the observed variation of each specimen, and heterogeneity for shale samples as reported in several

literatures, about 6 samples were tested for each fluid environment. The mean values and standard deviation were also computed and reported.

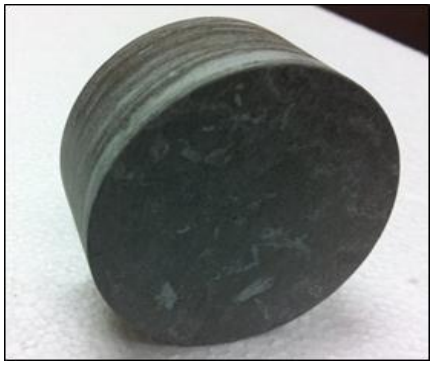

Fig. 3.10—Disc-shaped Mancos Shale Core

Fig. 3.11—Experimental Setup for Brazilian Test

3.8 Fracture Imaging Test

In order to characterize the effects of the fluid environment on the structural features of the shale core, it is necessary to have a visual observation of the fractures-both natural and induced present. The Universal Systems HD-350E X-Ray Computerized tomography (CT) scanner (shown in **Fig. 3.12)** was used to scan fractured cores before and after exposure to fluids being investigated. The presence of natural fractures is important because they control the deformation behavior of rocks. The overall mechanical properties of rock depend largely on its structural features.

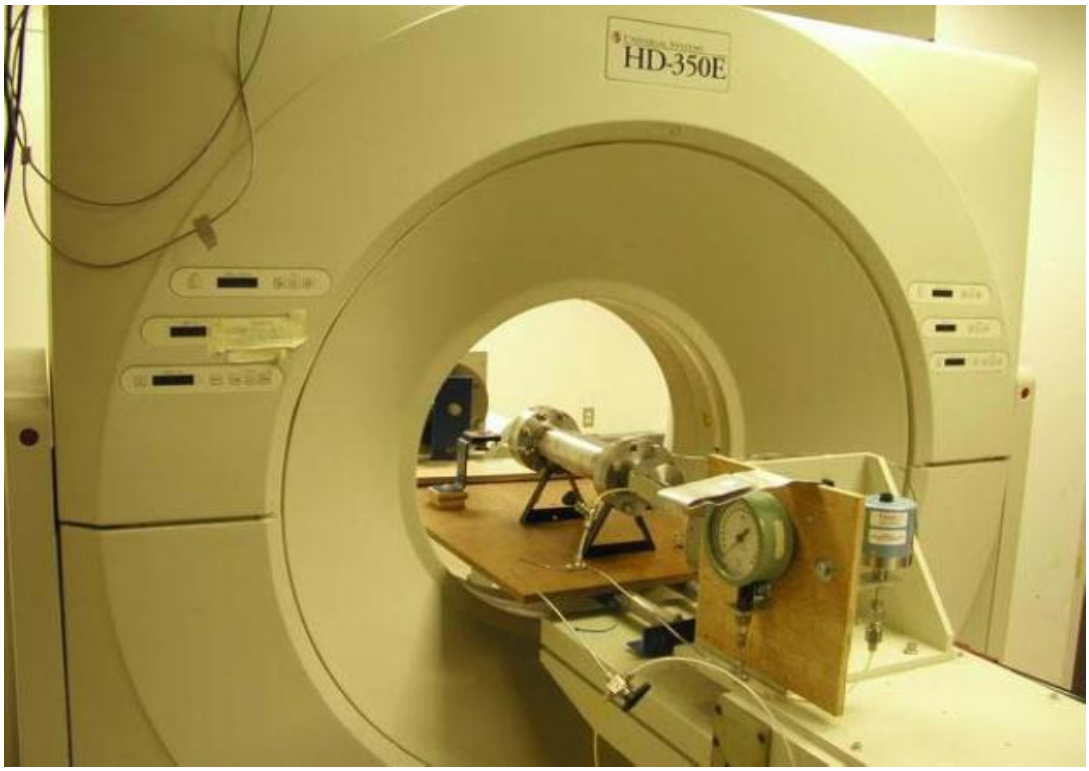

Fig. 3.12—Showing the Universal Systems HD-350E X-Ray CT Scanner

A system of test was designed to see the effects of fluid interaction after hydraulic fracturing and before flowback of fracture fluids. Cylindrical core samples were jacketed using heat shrink tubing and scanned to identify initial fractures present. The samples are loaded axially in the point load test system till fractures are created. The samples are scanned again to image the new fractures. The samples are then left in different solution systems- solution A- water, solution B- in 2.85×10^{-3} $mol.dm^{-3}$ cationic surfactant- DTAB and solution C- 2.81×10^{-3} $mol.dm^{-3}$ anionic surfactant- SDBS. The samples are scanned again after contact times of 4hours and 24 hours to observe the effect of the fluid systems on the created fractures.

CHAPTER IV

EXPERIMENTAL RESULTS, ANALYSES AND DISCUSSION

The results of the shale characterization and shale-fluid interaction tests are presented.

4.1 Mancos Shale Mineralogy Analysis

The minerals present in the rock gives a good indication of expected mineral dissolution, adsorption or desorption of the rock in the presence of different fluid environments. The XRD bulk pattern of the Mancos shale suggests the presence of quartz, calcite, dolomite, and the weak peak indicates the presence of clay minerals. In order to quantify the mineral composition, and identify the clay minerals, separation and clay fraction analysis was further carried out. The result of the analysis for the Mancos shale sample is presented in **Table 4.1.** The Mancos consists of relatively low clay (26%) and low smectite concentration, indicating that the Mancos shale at this cored depth has low shrink-swell capacity.

Table 4.1— Mineralogy of Mancos Shale Sample Cored at Depths of 20-60 ft.

		Composition, %	Totals, %
Clays	Chlorite	1	26
	Kaolinite	15	
	Illite/Mica	7	
	Mixed Layer Illite and Smectite	3	
Carbonates	Calcite	7	15
	Dolomite	8	
Other Minerals	Quartz	51	59
	K-Feldspar	3	
	Plagioclase	4	
	Pyrite	1	
	Fluoroapatite	Tr	
	Anhydrite and Barite	0	

4.2 Mancos Shale TOC and CEC Analysis

Initial fizz tests indicated that Mancos sample is a calcareous sample, the calcium carbonate equivalent was determined using the Chittick's apparatus while the total carbon was determined by dry combustion. The resulting difference of 0.85% is the total organic carbon in the Mancos shale sample studied.

In the CEC analysis, sodium acetate is used to identify possible sites for cation exchange. The tests were run four times, and the resulting average value for the sample was 7.4 Meq/100g. As mentioned in the previous chapter, the CEC of soil largely depends on its mineralogy. Kaolinite has the 1:1 structure, hence a relatively low CEC because the negative sites yet to be satisfied are only at the edge of the mineral. Organic

matter has a high CEC, therefore soil having a high percentage of organic matter have a relatively high CEC. Consequently, the low organic content and the absence of high CEC clays result in the low CEC determined for this shale sample. These results are summarized in **Table 4.2.**

Table 4.2— Soil Characterization of Mancos Shale Sample Cored at Depths of 20 ft. to 60 ft.

Cation Exchange Capacity, Meq/100g	7.4
Total Organic Carbon, %	0.85

4.3 Adsorption of Surfactants on Mancos Shale

In these tests, the change in surface tension is defined as the surfactant being adsorbed by the shale. An initial observation of the mixture after vigorous shaking was that the shale particles remained dispersed for a longer time in the anionic surfactant solution than in water and the cationic surfactant. **Fig. 3.6** shows the mixtures after about 4 hours of settling time. After 24 hours, the shale particles in the cationic surfactant appear to have settled faster, while in the anionic surfactant solution, there were still visibly-suspended fine solids.

The surface tension of the shale-surfactant mixture was higher than the initial surface tension of the solutions measured. Since the surfactants originally lower the

surface tension, the increase in surface tension occurs because there is less surfactant concentration present in the solution after equilibration with shale. The adsorption of either cationic or anionic surfactant at the solid-liquid interface is largely affected by the nature of charges on the surface (Muherei et al., 2009; Zhang et al., 2006).

Table 4.3—Change in Surface Tension with Shale Equilibration in Surfactant Solutions

	Molar Concentration, mol/liter	Surface Tension without shale, dynes/cm	Surface Tension with shale, dynes/cm	Change in Surface Tension, %
DTAB	2.85E-04	35.61	63.23	78
SDBS	2.81E-04	32.51	36.17	11

In the cationic surfactant solution system, at 2.85×10^{-4} $mol.dm^{-3}$, the solution is below the CMC. The surface tension of the solution was increased by about 80% after equilibration with shale as shown in **Table 4.3**. The loss of DTAB can be attributed to their adsorption to the negatively charged sites of organic matter and clay minerals present in the shale. Hence the adsorption mechanism is concluded to be electrostatic interaction. The neutralization of the negative sites on the shale surfaces reduces particle-particle interaction of suspended fine shale particles, leading to much more rapid settling of particles suspended in the DTAB solution than either in water or the SDBS solution.

In the anionic surfactant solution system, at 2.81×10^{-4} mol.dm^{-3}, the solution is below the CMC. The surface tension of the solution was increased by about 10% after equilibration with shale as shown in **Table 4.3**. The lower adsorption capacity of the SDBS can be attributed to electrostatic repulsion that exists between negatively charged shale surface and anionic nature of the surfactant. The electrostatic repulsion is also responsible for the long settling times for the fine shale particles suspended in the SDBS solution.

4.4 Uniaxial Compression Strength of Mancos Shale

The maximum load required to fail the cylindrical-shaped Mancos shale samples exposed to the different four fluid environments were determined from the unconfined compression experiments. The uniaxial compressive strength was calculated from the failure load using the following equation:

$$UCS = \frac{P}{A}. \quad \text{..... (4.1)}$$

where UCS is the uniaxial compressive strength

P is the maximum load required to fail the specimen

A is the specimen area

During the experiments, some samples fell apart on exposure to the aqueous environment particularly those exposed to water. These samples were not tested. Also samples with minor cracks were initially tested, but they yielded extremely low failure strengths because of the pre-existing fracture. The results from such tests were excluded from the statistical analysis. From the plot of the UCS for the shale samples in the

different environments in **Fig. 4.1**, the presence of aqueous environments influence the mechanical strength of the rock sample dry samples by the reduction in the rock strength. For the different aqueous environments, the strength of the samples appeared weakest on exposure to water, while the strength differences are not as distinct for the comparisons between anionic surfactants and cationic surfactant. **Table 4.4** summarizes the statistics of the test results.

Table 4.4— Uniaxial Compressive Strength of Mancos Shale Sample Cored at Depths of 20 to 60 ft.

UCS, psi	Dry Samples	Samples in Water	Samples in SDBS	Samples in DTAB
Mean	7,877	2,778	3,841	3,439
Standard deviation	1,105	647	1,648	1,311
Range	6489 - 9043	2164 - 3939	1857 - 6435	2468 - 5964
Count	5	6	6	6

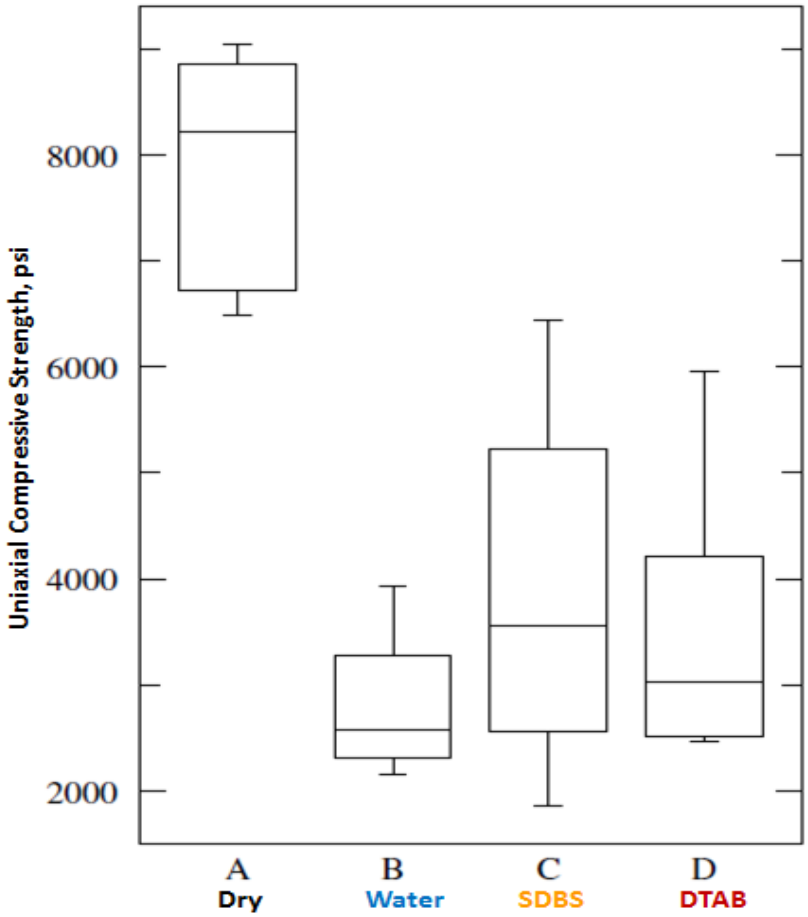

Fig. 4.1—Boxplot Showing Comparison of Uniaxial Compressive Strength (UCS) in Different Fluid Environments

4.5 Indirect Tensile Strength of Mancos Shale

The maximum load that generated enough tensile stress to split the disc-shaped Mancos shale samples exposed to the different four fluid environments was determined from the Brazilian experiments. The indirect tensile strength was calculated from the failure load using the following equation:

$$St = \frac{2P}{\pi t D}. \quad \text{..... (4.2)}$$

where St is the tensile strength

P is the maximum load required to fail the specimen

t is the specimen thickness

D is the specimen diameter

As mentioned for the unconfined compression test, during the experiments, some samples fell apart on exposure to the aqueous environment particularly those exposed to water. These samples were also discarded. The disc-shaped samples with minor cracks were initially tested, but they also yielded extremely low failure strengths because of the pre-existing fracture. Hence, such data were excluded from the statistical analysis. From the plot of the tensile strength of the shale samples in the different environments in **Fig. 4.2**, the presence of aqueous environments also influence the tensile strength of the rock sample dry samples by the reduction in the rock strength. For the different aqueous environments, there was not much distinction for the strength of the samples exposed to water and either surfactants**. Table 4.5** summarizes the statistics of the test results.

Table 4.5— Indirect Tensile Strength of Mancos Shale Sample Cored at Depths of 20 to 60 ft.

St, psi	Dry Samples	Samples in Water	Samples in SDBS	Samples in DTAB
Mean	1,038	689	691	650
Standard deviation	67	233	204	192
Range	969 - 1149	353 - 893	409 - 907	346 - 900
Count	5	5	7	7

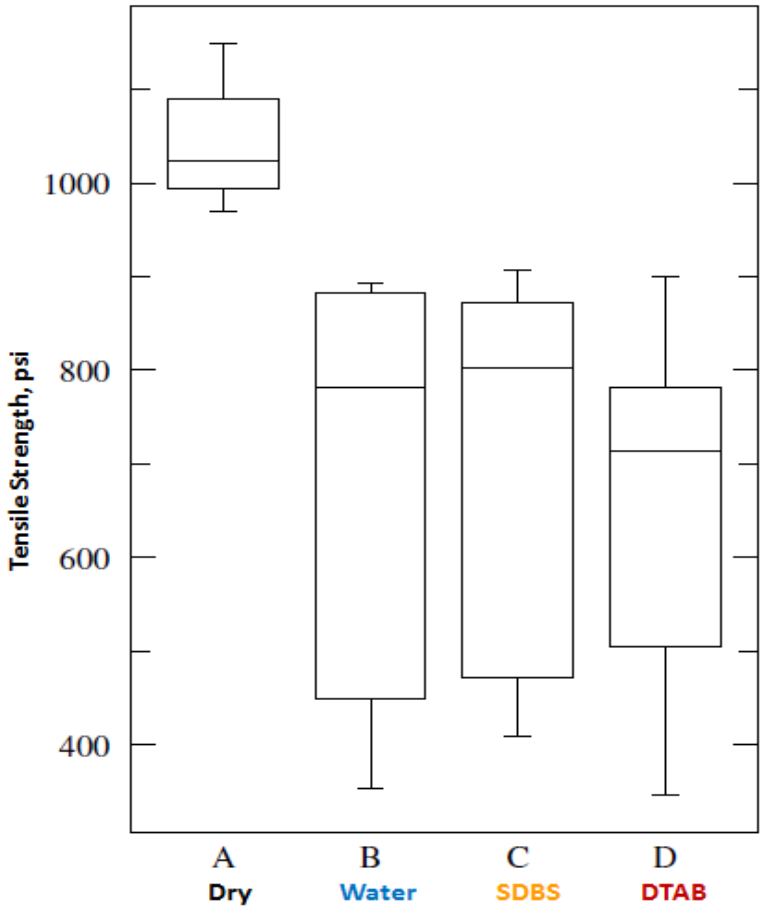

Fig. 4.2— Boxplot Showing Comparison of Tensile Strength (St) in Different Fluid Environments

4.6 Test of Hypothesis

The hypothesis of this work is that the strengths required to fail the Mancos shale samples either in compression or tension would vary with the different fluid environment. According to Seto et al. (1997), the reduction in hardness of rock as a result of adsorption is known as the Rehbinder effect. This hypothesis was tested using

analysis of variance (ANOVA) for the sets of data. A significance level, α of 0.05 was assumed. The null hypothesis (H_0) is stated as follows (Montgomery, 2011):

$$H_{0:}\ \mu_1 - \mu_0 = \Delta_0. \quad \text{..... (4.3)}$$

The alternative hypothesis (H_1) is stated as

$$H_{1:}\ \mu_1 - \mu_0 \neq \Delta_0. \quad \text{..... (4.4)}$$

Δ_0 is assumed to be zero, hence, the equality of the means are tested.

The results showed that the null hypothesis cannot be accepted since the probability for the result is less than 0.0001 ($p<0.0001$) for the uniaxial compressive strength tests and less than 0.0096 ($p<0.0096$) for the indirect tensile strength tests. The ANOVA test was followed by t-tests to determine which of the data sets were statistically different. Since this requires multi-pairwise comparisons, it is necessary to correct the significance level to ensure that the overall experiment-wise significant level remains the same. This was done using the Bonferroni adjustment, where the new significance level is defined as 'α/number of tests' (Weisstein).

The t-tests were carried out comparing the following 6 cases:

- Case A: Dry samples vs. Samples in water
- Case B: Dry samples vs. Samples in cationic surfactant (DTAB)
- Case C: Dry samples vs. Samples in anionic surfactant (SDBS)
- Case D: Samples in water vs. Samples in cationic surfactant (DTAB)
- Case E: Samples in water vs. Samples in anionic surfactant (SDBS)
- Case F: Samples in anionic surfactant (SDBS) vs. Samples in cationic surfactant (DTAB)

With no correction, the chance of finding one or more significant differences in the 6 tests is 0.2649 (26.49%). Hence, α is adjusted to 0.008.

The sample variances are combined by a weighted average and expressed as s_p^2 as shown in the following equation:

$$s_p^2 = \frac{(n_1 - 1)s_1^2 + (n_2 - 1)s_2^2}{n_1 + n_2 - 2} \quad . \quad \text{..... (4.5)}$$

where $n_1 + n_2 - 2$ represents the degree of freedom.

The t-statistic is computed as follows:

$$t_0 = \frac{\overline{x_1} - \overline{x_2} - (\mu_1 - \mu_2)}{s_p\sqrt{\frac{1}{n_1} + \frac{1}{n_2}}} \quad . \quad \text{..... (4.6)}$$

where $\overline{x}$ represents the mean of the population.

The results of the t-tests are summarized in **Table 4.6** and **Table 4.7** for the unconfined compression tests and Brazilian tests respectively. For both mechanical properties- uniaxial compressive strength and tensile strength, the null hypothesis is rejected when comparing the strengths of dry samples with samples exposed to any of the aqueous environment. Hence, the significant reduction in the mechanical strengths of the shale can be attributed to their exposure to water, cationic or anionic surfactant.

Also from the analysis, when comparing the mechanical properties of the shale on exposure to the three aqueous environments, the null hypothesis is accepted. Hence for the concentrations of cationic and anionic surfactants used, there is no statistical difference in the strengths of the shale failed in either the compression or tension mode

when exposed to water, cationic or anionic surfactant. The compressive strengths of the samples had comparative means of 2778 psi, 3841 psi and 3439 psi when exposed to water, anionic surfactant and cationic surfactant respectively, while the tensile strengths of the samples had comparative means of 689 psi, 691 psi and 650 psi when exposed to water, anionic surfactant and cationic surfactant respectively.

Table 4.6—Summary of Test of Means Analysis for Mancos Shale Samples Failed in Compression Mode.

Cases	Degree of freedom	Level of significance	s_p	t_o	t-distribution	Hypothesis
A	10	0.008	996.67	9.29	3.28	H_1
B	10	0.008	969.18	9.76	3.28	H_1
C	8	0.008	905.21	11.67	3.48	H_1
D	12	0.008	892.91	0.24	3.15	H_0
E	10	0.008	786.71	2.62	3.28	H_0
F	11	0.008	786.71	2.49	3.28	H_0

Table 4.7—Summary of Test of Means Analysis for Mancos Shale Samples Failed in Tension Mode.

Cases	Degree of freedom	Level of significance	s_p	t_o	t-distribution	Hypothesis
A	12	0.008	278.91	4.67	3.15	H_1
B	13	0.008	244.95	5.68	3.11	H_1
C	13	0.008	244.30	6.55	3.11	H_1
D	11	0.008	174.86	0.17	3.21	H_0
E	11	0.008	173.79	1.29	3.21	H_0
F	12	0.008	122.03	1.65	3.15	H_0

4.7 X-ray Computerized Tomography (CT) Analysis

The images of the shale samples after initial fracture, exposure to fluid for 4 and 24 hours respectively are shown in **Fig. 4.3**. Although the surfactants were expected to travel into the matrix, the images do not show clear distinction between induced fractures and the resulting fractures or microfractures after exposure to fluids. Other than the images the CT number response of the samples in different fluid environment were studied. The CT number represents the intensity resulting from the attenuation of photons which is correlated to the density of the object. The CT number increases with exposure time as shown in **Fig. 4.4**. The change in CT number response was a bit higher in water compared to the surfactants.

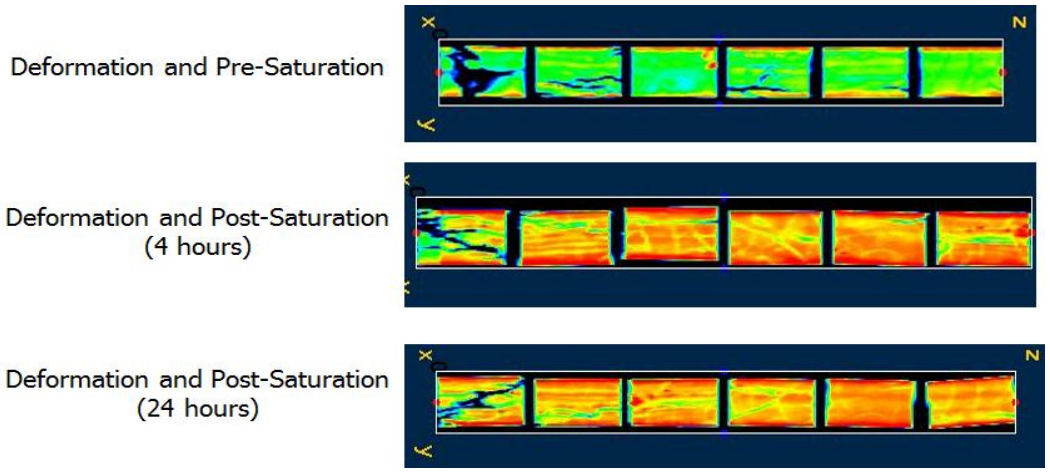

Fig. 4.3—Image of Fractured Cores in CT Scan

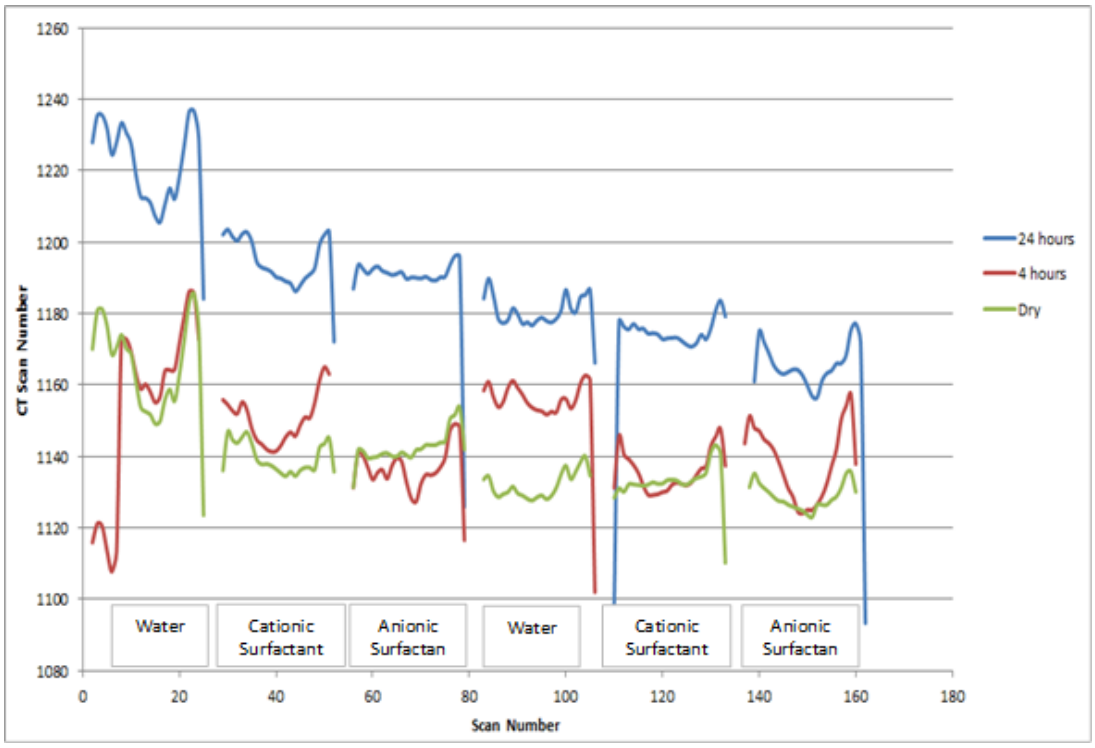

Fig. 4.4—CT Number Response of Fractured Shale in Aqueous Environments

CHAPTER V

CONCLUSIONS

5.1 Summary

1. The experimental design using unconfined compression platens and Brazilian test loading jaws fitted into GCTS compression frames for determination of uniaxial compression strength and indirect tensile strength respectively showed good agreement with other equipment used in determining these properties.
2. The low CEC of the Mancos shale studied can be attributed to the low organic matter and absence of high CEC clays.
3. Adsorption tests show the chemical interaction between the surfactant solution and the shale. The equilibrium mixture of shale and DTAB show a significant increase (80%) in surface tension of the initial DTAB solution. This indicates loss of the surfactant solution to the shale surface. The probable sorption mechanism is electrostatic attraction between negatively charged sites of the shale (organic matter and clay minerals). This cationic surfactant clearly adsorbs moderately to strongly to Mancos shale surface.
4. The equilibrium mixture of shale and SDBS show only about 10% increase in surface tension indicating minor adsorption of this anionic surfactant to the shale.
5. Despite the relatively low clay and low swelling clay content of the Mancos shale, the mechanical strength is influenced by exposure to aqueous environments. From the statistical analysis, for a comparison between dry samples and samples in

aqueous environment, both properties of the rock- uniaxial compressive strength and tensile strength demonstrate sensitivity on exposure to water, cationic surfactant and anionic surfactant.

6. Based on the number of tests carried out and the concentration of both cationic and anionic surfactants used, the compressive strengths of the samples had comparative average compressive strengths of 2778 psi, 3841 psi and 3439 psi when exposed to water, anionic surfactant and cationic surfactant respectively. Using the Bonferroni correction in a test of means analysis, the nature of chemical solutions does not result in a significant statistical difference in compressive strengths. Simply wetting with water is sufficient to explain loss of compressive strength in all cases.
7. Similarly, based on the number of tests carried out and the concentration of surfactants used, the tensile strengths of the samples had comparative average compressive strengths of 689 psi, 691 psi and 650 psi when exposed to water, anionic surfactant and cationic surfactant respectively. Using the Bonferroni correction in a test of means analysis, the nature of chemical solutions does not result in a significant statistical difference when failed in tensile mode. Again, simply wetting with water is sufficient to explain loss of tensile strength in all cases.
8. Due to the limited number of tests and very heterogeneous nature of the Mancos shale, a strong conclusion cannot be drawn on the difference in the effect of chemical solutions on the mechanical property of shale samples.

9. The images from the CT scan do not show clear distinction between induced fractures and the resulting fractures or microfractures after exposure to fluids. No clear-cut conclusions can be made from the changes in CT number responses.

5.2 Recommendations/Future Work

1. A larger number of tests using experimental design would be required to define a distinct difference of the reaction of shale with the aqueous systems. This could include: :
    a. testing at a higher concentration or range of surfactant concentrations
    b. effect of introducing shale stabilizer to determine if the large losses of compressive and tensile strength of shale samples can be mediated by such materials. Further experiments to evaluate effects of 2% KCl or polymeric clay stabilizers are warranted.
    c. knowledge of zeta potential of the suspended shale particles and their changes and any effect in the presence of surfactants and clay stabilizer.
2. Design of tests using hollow cylinders and tests that measure changes in fracture toughness, ultrasonic velocity and crack propagation stress and simulation of downhole in-situ stress conditions would also be beneficial to these studies.

REFERENCES

Ananda, K., Yadav, O.P., and Singh, P.P. 1991. Studies on the Surface and Thermodynamic Properties of Some Surfactants in Aqueous and Water+1,4-Dioxane Solutions. *Colloids and Surfaces* **55** : 345-358.

Atkinson, B.K. 1982. Subcritical Crack Propagation in Rocks: Theory, Experimental Results and Applications. *Journal of Structural Geology* **4** (1): 41-56.

Atkinson, B.K. 1987. Fracture Mechanics of Rock Edited by Barry Kean Atkinson. *Academic Press Geology Series*:117-125. London: Elsevier. 978-0-12-066265-4

Corrêa, C.C. and Nascimento, R.S.V. 2005. Study of Shale-Fluid Interactions Using Thermogravimetry. *Journal of Thermal Analysis & Calorimetry* **79** (2): 295-298. 16184094.

Deng, Y.J., Dixon, J.B., and White, G.N. 2006a. Adsorption of Polyacrylamide on Smectite, Illite, and Kaolinite. *Soil Science Society of America Journal* **70** (1): 297-304.

Deng, Y.J., Dixon, J.B., and White, G.N. 2006b. Bonding Mechanisms and Conformation of Poly(Ethylene Oxide)-Based Surfactants in Interlayer of Smectite. *Colloid and Polymer Science* **284** (4): 347-356.

Dunning, J.D., Lewis, W.L., and Dunn, D.E. 1980. Chemomechanical Weakening in the Presence of Surfactants. *J. Geophys. Res.* **85** (10): 5344-5354. OSTI ID: 6092193.

Harrison, J.P. and Hudson, J.A. 2000. *Engineering Rock Mechanics: An Introduction to the Principles*. Materials & Mechanical. Imperial College of Science, Technology and Medicine. University of London, UK.: Elsevier. 978-0-08-043864-1

Huang, Z., Yan, Z., and Gu, T. 1989. Mixed Adsorption of Cationic and Anionic Surfactants from Aqueous Solution on Silica Gel. *Colloids and Surfaces* **36** (3): 353-358.

Jaeger, J.C., Cook, N.G.W., and Zimmerman, R.W. 2007. *Fundamentals of Rock Mechanics* 4th: John Wiley & Sons.

Karfakis, M.G. and Akram, M. 1993. Effects of Chemical Solutions on Rock Fracturing. *International Journal of Rock Mechanics and Mining Sciences & Geomechanics Abstracts* **30** (7): 1253-1259.

Kaufman, P.B., Penny, G.S., and Paktinat, J. 2008. Critical Evaluation of Additives Used in Shale Slickwater Fracs. Paper presented at the SPE Shale Gas Production Conference, Fort Worth, Texas, USA. Society of Petroleum Engineers 119900.

Lewis, W.L. 1976. Effect of Aqueous Surfactants on Crack Propagation Rate in Crab Orchard Sandstone. *North Carolina Univ, Chapel Hill, Ph.D Thesis* (197751).

Montgomery, D.C. 2011. *Applied Statistics and Probability for Engineers /Douglas C. Montgomery, George C. Runger.* 5th ed. Hoboken, N.J.: John Wiley & Sons.

Muherei, M.A., Junin, R., and Bin Merdhah, A.B. 2009. Adsorption of Sodium Dodecyl Sulfate, Triton X100 and Their Mixtures to Shale and Sandstone: A Comparative Study. *Journal of Petroleum Science and Engineering* **67** (3-4): 149-154.

Rodríguez-Cruz, M.S., Sanchez-Martin, M.J., and Sanchez-Camazano, M. 2005. A Comparative Study of Adsorption of an Anionic and a Non-Ionic Surfactant by Soils Based on Physicochemical and Mineralogical Properties of Soils. *Chemosphere* **61** (1): 56-64.

Sánchez-Martín, M.J., Dorado, M.C., del Hoyo, C. and Rodríguez-Cruz, M. S. 2008. Influence of Clay Mineral Structure and Surfactant Nature on the Adsorption Capacity of Surfactants by Clays. *Journal of Hazardous Materials* **150** (1): 115-123.

Santos, H., Diek, A., da Fontoura, S. and Roegiers, J.C. 1997. Shale Reactivity Test: A Novel Approach to Evaluate Shale-Fluid Interaction. *International Journal of Rock Mechanics and Mining Sciences* **34** (3-4): 268.

Schumacher, B.A. 2002. Methods for the Determination of Total Organic Carbon (TOC) in Soils and Sediments. In, ed. Office of Research and Development, L.V.

Seto, M., Nag, D.K., Vutukuri, V.S. and Katsuyama, K. 1997. Effect of Chemical Additives on the Strength of Sandstone. *International Journal of Rock Mechanics and Mining Sciences* **34** (3-4): 280.

Shchukin, E.D., Pertsov, A.V., Amelina, E.A. and Zelenev, A.S. 2001. *Colloid and Surface Chemistry*. 1st. Chemical, Petrochemical & Process: Elsevier. 978-0-44-450045-8.

Weisstein, E.W. "Bonferroni Correction." From Mathworld --a Wolfram Web Resource. http://mathworld.wolfram.com/BonferroniCorrection.html.

Zelenev, A.S. 2011. Surface Energy of North American Shales and Its Role in Interaction of Shale with Surfactants and Microemulsions. Paper presented at the SPE International Symposium on Oilfield Chemistry, The Woodlands, Texas, USA. Society of Petroleum Engineers 141459.

Zhang, M.-N., Liao, X.-P., and Bi, S. 2006. Adsorption of Surfactants on Chromium Leather Waste. *Journal of the Society of Leather Technologists and Chemists, China;* **90**: 1-6.

Zhang, R. and Somasundaran, P. 2006. Advances in Adsorption of Surfactants and Their Mixtures at Solid/Solution Interfaces. *Advances in Colloid and Interface Science* **123-126**: 213-229.

APPENDIX

Table A1—Results Recorded from Unconfined Compression Tests

	Failure Strength, kN	Uniaxial Compessive Strength, MPa	Uniaxial Compessive Strength, psi
Samples in air (dry)			
1BDRY	22.85	44.74	6489
2BDRY	24.51	47.99	6961
3BDRY	28.91	56.61	8210
4BDRY	30.57	59.86	8682
5BDRY	31.84	62.35	9043
Samples in water			
1BWAT	7.62	14.92	2164
2BWAT	8.30	16.25	2357
3BWAT	8.59	16.82	2440
4BWAT	9.57	18.74	2718
5BWAT	10.74	21.03	3050
6BWAT	13.87	27.16	3939
Samples in anionic surfactant (SDBS)			
1BANI	6.54	12.81	1857
2BANI	9.86	19.31	2800
3BANI	10.45	20.46	2968
4BANI	14.65	28.69	4161
5BANI	16.99	33.27	4825
6BANI	22.66	44.37	6435
Samples in cationic surfactant (DTAB)			
1BCAT	8.69	17.02	2468
2BCAT	8.89	17.41	2525
3BCAT	10.06	19.70	2857
4BCAT	11.23	21.99	3189
5BCAT	12.79	25.04	3632
6BCAT	21.00	41.12	5964

Table A2—Results Recorded from Brazilian Tests

	Failure Strength, kN	Tensile Strength, MPa	Tensile Strength, psi
Samples in air (dry)			
1ADRY	13.63	6.68	969
2ADRY	14.32	7.02	1018
3ADRY	14.41	7.06	1024
4ADRY	14.51	7.11	1031
5ADRY	16.17	7.92	1149
Samples in water			
1AWAT	4.97	2.44	353
2AWAT	7.69	3.77	547
3AWAT	11.00	5.39	782
4AWAT	12.27	6.01	872
5AWAT	12.56	6.16	893
Samples in anionic surfactant (SDBS)			
1AANI	5.75	2.82	409
2AANI	6.62	3.24	471
3AANI	7.99	3.92	568
4AANI	11.30	5.54	803
5AANI	11.39	5.58	810
6AANI	12.27	6.01	872
7AANI	12.76	6.25	907
Samples in cationic surfactant (DTAB)			
1ACAT	4.87	2.39	346
2ACAT	7.11	3.48	505
3ACAT	7.60	3.72	540
4ACAT	10.03	4.92	713
5ACAT	10.71	5.25	761
6ACAT	11.00	5.39	782
7ACAT	12.66	6.20	900

VITA

Name: Aderonke Abiodun Aderibigbe

Address: Department of Petroleum Engineering
Texas A&M University
3116 TAMU - 501 Richardson Building
College Station, TX, 77843-3116

Email Address: ronkeaderibigbe@gmail.com

Education: B.Sc., Chemical Engineering, University of Lagos, Nigeria, 2006
M.Sc., Petroleum Engineering, Texas A&M University, 2012